Helsingin Yliopiston Maantieteen Laitoksen Julkaisuja
Publicationes Instituti Geographici Universitatis Helsingiensis
A 147

Remote sensing of leaf area index: enhanced retrieval from close-range and remotely sensed optical observations

Alemu Gonsamo Gosa

Remote sensing of leaf area index: enhanced retrieval from close-range and remotely sensed optical observations

Alemu Gonsamo Gosa

Department of Geography
Faculty of Science
University of Helsinki
Finland

Academic dissertation

To be presented, with the permission of the Faculty of Science of the University of Helsinki, for public criticism in the Auditorium XII, Main Building, Fabianinkatu 33, on December 18th 2009, at 10 o'clock.

Helsinki 2009

Supervisor: Dr. Petri Pellikka
Professor
Department of Geography
University of Helsinki
Finland

Pre-examiners: Dr. Pauline Stenberg
Professor
Department of Forest Resource Management
University of Helsinki
Finland

Dr. Tiit Nilson
Senior research associate, Professor
Department of Atmospheric Physics
Tartu Observatory
Estonia

Opponent: Dr. Jing Ming Chen
Senior Canada Research Chair, Professor
Department of Geography and Program in Planning
University of Toronto
Canada

Publisher:
Department of Geography
Faculty of Science
PO Box 64, FI-00014 University of Helsinki
Finland

ISBN 978-952-10-5872-1 (pbk)
ISBN 978-952-10-5873-8 (PDF)
ISSN 0300-2934
http://ethesis.helsinki.fi

Hansaprint - Hansa Direct 2009
Helsinki 2009

To my family

ABSTRACT

A wide range of models used in agriculture, ecology, carbon cycling, climate and other related studies require information on the amount of leaf material present in a given environment to correctly represent radiation, heat, momentum, water, and various gas exchanges with the overlying atmosphere or the underlying soil. Leaf area index (LAI) thus often features as a critical land surface variable in parameterisations of global and regional climate models, e.g., radiation uptake, precipitation interception, energy conversion, gas exchange and momentum, as all areas are substantially determined by the vegetation surface. Optical wavelengths of remote sensing are the common electromagnetic regions used for LAI estimations and generally for vegetation studies.

The main purpose of this dissertation was to enhance the determination of LAI using close-range remote sensing (hemispherical photography), airborne remote sensing (high resolution colour and colour infrared imagery), and satellite remote sensing (high resolution SPOT 5 HRG imagery) optical observations. The commonly used light extinction models are applied at all levels of optical observations. For the sake of comparative analysis, LAI was further determined using statistical relationships between spectral vegetation index (SVI) and ground based LAI. The study areas of this dissertation focus on two regions, one located in Taita Hills, South-East Kenya characterised by tropical cloud forest and exotic plantations, and the other in Gatineau Park, Southern Quebec, Canada dominated by temperate hardwood forest.

The sampling procedure of sky map of gap fraction and size from hemispherical photographs was proven to be one of the most crucial steps in the accurate determination of LAI. LAI and clumping index estimates were significantly affected by the variation of the size of sky segments for given zenith angle ranges. On sloping ground, gap fraction and size distributions present strong upslope/downslope asymmetry of foliage elements, and thus the correction and the sensitivity analysis for both LAI and clumping index computations were demonstrated. Several SVIs can be used for LAI mapping using empirical regression analysis provided that the sensitivities of SVIs at varying ranges of LAI are large enough. Large scale LAI inversion algorithms were demonstrated and were proven to be a considerably efficient alternative approach for LAI mapping. LAI can be estimated nonparametrically from the information contained solely in the remotely sensed dataset given that the upper-end (saturated SVI) value is accurately determined. However, further study is still required to devise a methodology as well as instrumentation to retrieve on-ground 'green leaf area index'. Subsequently, the large scale LAI inversion algorithms presented in this work can be precisely validated. Finally, based on literature review and this dissertation, potential future research prospects and directions were recommended.

Keywords: airborne CIR image, airborne colour image, clumping index, forest, hemispherical photography, high resolution optical satellite image, large scale leaf area index inversion, leaf area index, slope correction

ACKNOWLEDGEMENTS

I would like to thank my supervisor Prof. Petri Pellikka for providing me an opportunity to work in the Geoinfomatics Research Group. I am grateful for the independence, sufficient freedom, responsibilities and friendly working environment he has given me during my dissertation work.

I am particularly thankful to Prof. Jean-Michel N Walter, who was so kind and patient with all my hastily written emails. I have learned a lot from you.

Prof. Doug J King has been a co-author in one of my papers. Thank you very much for the hospitality during the field visit to Gatineau Park.

Dr. Richard Fernandes has shared brief scientific and general discussions. It reaffirmed my confidence every time when I talked to you.

I am also grateful to pre-examiners, Prof. Pauline Stenberg and Prof. Tiit Nilson for reviewing this work and providing constructive criticism.

I am thankful to Prof. Pauline Stenberg and Prof. Doug J King for the digital cameras and fish-eye lenses.

The friendly and supportive atmosphere inherent to the Department of Geography, University of Helsinki contributed essentially to the final outcome of my dissertation. Prof. John Westerholm, Johanna Jaako and Airi Töyrymäki have been very welcoming, warm and supportive for all administrative matters. Thanks to students, staff and visiting scholars of the Department of Geography, University of Helsinki for the enjoyable times. I am also deeply respectful for the support in IT issues from Tom Blom and Hilkka Ailio. Particularly, the support from Tom Blom essentially contributed to the efficiency of my dissertation.

Dr. Tuuli Toivonen, Dr. Gabriela Schaepman, Dr. Inge Jonckheere, Dr. Tino Johansson, and Dr. Jon Pasher deserve special thanks for various reasons.

Thanks to Mr. Mika Siljander, Mr. Barnaby Clark, Dr. Janne Heiskanen, Dr. Jan Hjort, and Ms. Nina Himberg for keeping the office life lively, having discussion ranging from scientific to the most ridiculous ones and for the good times. Also thanks to Barnaby for proof reading of some of the articles.

I owe my loving thanks to Petra D'Odorico. Her splendid love, intelligence, goodness, and liveliness have supported me in hundreds of ways throughout the development and writing of this dissertation. Petra has been crucial for my mental coherence during the entire dissertation process. Without her I would have probably ended up insane by overworking.

Special thanks go to my family, for their support, love and encouragement. They have given their unconditional support, knowing that doing so contributed greatly to my absence these last post-high-school years. They were strong enough to let me go easily, to believe in me, to hold back all family issues from conversation for my comfort, and to let slip away all those years during which we could have been geographically closer.

The financial support of the Centre for International Mobility (CIMO), Academy of Finland through TAITATOO (pr. no. 110294) project and personal grants to Prof. Pellikka (pr. no. 21252), Department of Geography of University of Helsinki, Finnish Graduate School of Geography, University of Helsinki Chancellor's grant, Natural Sciences and Engineering Research Council through grant to Prof. King, EuroDIVERSITY project from European Science Foundation, and OASIS financed by the European Commission (DG Research) are gratefully acknowledged.

I apologise to those that I forgotten to mention here.

LIST OF ORIGINAL ARTICLES

This dissertation consists of an introductory review followed by seven Papers, which are referred to in the text by their Roman numerals. The articles are reprinted with kind permission of the publishers. Some of the articles contain colour figures, which have been printed here in greyscale.

I. **Gonsamo A**, J-MN Walter & P Pellikka. Sampling gap fraction and size for estimating leaf area and clumping indices using hemispherical photography. *Canadian Journal of Forest Research*, submitted for publication.

II. **Gonsamo A** & P Pellikka (2008). Methodology comparison for slope correction in canopy leaf area index estimation using hemispherical photography. *Forest Ecology and Management* 256, 749─759.

III. **Gonsamo A** & P Pellikka (2009). The computation of foliage clumping index using hemispherical photography. *Agricultural and Forest Meteorology* 149, 1781─1787.

IV. **Gonsamo A** & P Pellikka. The sensitivity of spectral vegetation indices to Leaf Area Index. *IEEE Journal of Selected Topics in Earth Observations and Remote Sensing*, submitted for publication.

V. **Gonsamo A**, P Pellikka & DJ King (2009). Large scale leaf area index inversion algorithms from high resolution airborne imagery. *International Journal of Remote Sensing*, in press.

VI. **Gonsamo A** & P Pellikka (2009). A new look at top-of-canopy gap fraction measurements from high-resolution airborne imagery. *EARSeL eProceedings* 8, 64─74.

VII. **Gonsamo A**. Leaf area index retrieval using gap fractions obtained from high resolution satellite data: comparisons of approaches, scales and atmospheric effects. *International Journal of Applied Earth Observation and Geoinformation*, submitted for publication.

AUTHOR'S CONTRIBUTION

I am solely responsible for the planning of field studies and the research Papers, carrying out statistical and data analysis, and writing all research Papers listed above. Dr. Jean-Michel N Walter has pre-reviewed Paper I. Dr. Doug J King has pre-reviewed Paper V. Dr. Petri Pellikka has participated in the field data collection and setup.

SYMBOLS AND ABBREVIATIONS

β	Ground slope angle
ε_U	Unintercepted photon
ε_T	Scattered forward/transmitted photon
ε_A	Absorbed photon
ε_R	Scattered backward/reflected photon
φ	Azimuth angle
γ	Incidence angle
π	A mathematical constant (Pi) whose value is the ratio of any circle's circumference to its diameter in Euclidean space (3.14159)
θ	Zenith angle
ρ_{HS}	Hotspot reflectance
ρ_{DS}	Darkspot reflectance
Ω	Markov parameter (clumping index)
$\mu g.cm^{-2}$	Microgram per square centimetre
μm	Micrometre
1D	One dimensional
2D	Two dimensional
3D	Three dimensional
6S	Second simulation of the satellite signal in the solar spectrum
a	Slope of the regression of K against θ
A	Ground surface area
b	Intercept of the regression of K against θ
f_c	Fractional vegetation cover
Fc	Fractional clumping
g	Layer thickness or the binomial clumping index
G	Mean projection of a unit leaf area in the direction of the beam and onto a plane normal to the beam
$g.cm^{-2}$	Gram per square centimetre
Gt	Gigatonne
k	Ellipsoidal extinction coefficient
K	Mean contact number
km	Kilometre
L	Projected leaf area of a canopy
ln	Natural logarithm
m	Metre
n	Number of zenith angles
N	Number of layers
nm	Nanometre
P	Gap fraction (a probability of non-interception)
r	Reflectance
R	Relative sensitivity
S	Sensitivity function
x	Ellipsoidal shape parameter

ALIA	Average leaf inclination angle
ARVI	Atmospherically resistant vegetation index
AVHRR	Advanced very high resolution radiometer
BRDF	Bidirectional reflectance distribution function
CCA	Canonical correlation analysis
CCD	Charge-coupled device
CCOS	Global climate observing system
CDED	Canadian digital elevation data
CEOS	Committee on Earth observation satellites
CEOS-WGCV	CEOS working group on calibration and validation
CIR	Colour infrared
CYCLOPES	Cycle and change in land observational products from an ensemble of satellites
DART	Discrete anisotropic radiative transfer
DEM	Digital elevation model
DOS	Dark object subtraction
DVI	Difference vegetation index
ENVISAT	Environmental satellite
ESA	European space agency
EVI	Enhanced vegetation Index
exp	Exponential function with the base number approximately 2.718
FPAR	Fraction of photosynthetically active radiation
GCP	Ground control point
GORT	Geometric-optical radiative transfer
GPS	Global position system
GTOS	Global terrestrial observing system
HDS	Hot–dark spot index
HDF	Hierarchical data format
ISR	Infrared simple ratio
LAD	Leaf angle distribution
LAI	Leaf area index
LEAFMOD	Leaf Experimental Absorptivity Feasibility MODel
LIBERTY	Leaf incorporating biochemistry exhibiting reflectance and transmittance yields
LIDAR	Light detection and ranging
LPV	Land product validation
LSA SAF	Land surface analysis satellite applications facility
LSR	Least square regression
MCRT	Monte Carlo ray tracing
MERIS	Medium resolution imaging spectrometer
MISR	Multiangle imaging spectroradiometer
MODIS	Moderate resolution imaging spectroradiometer
MSAVI	Modified soil-adjusted vegetation index
MSR	Modified simple ratio
NAD83	North American datum 1983
NASA	National aeronautics and space administration
NCAR CCM3	National center for atmospheric research community climate model
NCC	National capital commission
NDHD	Normalized difference between hotspot and darkspot
NDII	Normalized difference infrared index

NDVI	Normalized difference vegetation index
NIR	Near infrared
NOAA	National oceanic and atmospheric administration
OAA	Overall average accuracy
PAR	Photosynthetically active radiation
PCA	Principal component analysis
POLDER	POLarization and Directionality of the Earth's Reflectances
POSTEL	Pôle d'Observation des Surfaces continentales par TELédétection
PROSAIL	Coupled SAIL and PROSPECT model
PVI	Perpendicular vegetation index
RADAR	Radio detection and ranging
RAMI	RAdiation transfer Model Intercomparison
REN	Relative equivalent noise
RISR	Reduced infrared simple ratio
RMSE	Root mean squared error
RNDVI	Reduced normalized difference vegetation Index
ROMC	RAMI on-line model checker
RSR	Reduced simple ratio
SAIL	Scattering by arbitrary inclined leaves
SAVI	Soil adjusted vegetation index
SDVI	Scaled difference vegetation index
SLOP	Stochastic model for leaf optical properties
SPOT HRG	Satellite Pour l'Observation de la Terre High Resolution Geometric
SR	Simple ratio
SVI	Spectral vegetation index
SVI_{∞}	SVI value for infinite LAI (asymptotic value)
SVI_{back}	SVI value for the soil (LAI = 0)
SWIR	Shortwave infrared
TRAC	Tracing radiation and architecture of canopies
TSAVI	Transformed soil adjusted vegetation index
UTM	Universal transverse mercator
VEN	Vegetation equivalent noise
WDVI	Weighted difference vegetation index
WIST	Warehouse inventory search tool

CONTENTS

1. INTRODUCTION

1.1 Optical remote sensing of vegetation

Remote sensing of the Earth, using instruments other than the naked eye, began in 1859 with Gaspard Tournachon's photograph from a balloon of a village near Paris, France (Goetz *et al.* 1985). Remote sensing is a science and an art of the small or large-scale acquisition of information of an object or phenomenon, by the use of either recording or real-time sensing devices that are not in physical or intimate contact with the object, such as by way of close-range, aircraft, spacecraft, satellite, buoy, or ship (Barrett & Curtis 1976; Lintz & Simonett 1976). The term remote sensing as usually defined, and as defined in this dissertation, applies for Earth observation such that information is acquired about Earth's land and water surfaces (Campbell 2002). The atmosphere is usually considered to be a hindrance rather than an object of investigation (Goetz *et al.* 1985). Remote sensing deals with the detection and measurement of phenomena or an object with devices sensitive to electromagnetic energy such as cameras and scanners for light, thermal scanners for heat, and radar for radio waves. The basic components to record or measure the remotely sensed data include the energy source, the transmission path, the target and the sensor. Based on the energy source, remote sensing can be passive or active sensing of information (White 1977). Passive sensors detect natural radiation that is emitted or reflected by the object or surrounding area being observed using reflected sunlight as a common source of radiation. Passive sensors include film photography, infrared, charge-coupled devices (CCD), and radiometers. Active sensors, on the other hand, emit energy in order to scan objects and areas whereupon a sensor then detects and measures the radiation that is reflected or backscattered from the target. Radio detection and ranging (RADAR) is an example of active remote sensing where the time delay between emission and return is measured, establishing the location, height, speed and direction of an object. Light detection and ranging (LIDAR) is another active source remote sensing technique, which is similar to radar but uses a laser instead of radio waves to produce detailed topographic maps and images.

Electromagnetic energy reaching the Earth's surface from the sun is either reflected (scattered), transmitted or absorbed. A basic assumption made in remote sensing is that specific targets such as soils of different types, water with varying degrees of impurities, rocks of differing lithologies, or vegetation of various species have an individual and characteristic manner of interacting with incident radiation that is described by the spectral response of that target (Figure 1). The spectral response of a target also depends upon such external factors as the zenith and azimuth angles of the sun, direction in which the sensor is pointing relative to nadir (the look angle), the topographic position of the target in terms of slope orientation, and the state of the atmosphere. The spectral reflectance curve is affected by factors such as soil nutrient status, the state of health and phenology of vegetation, and the colour of the soil (which may be affected by recent weather conditions). In some instances, the nature of the interaction between incident radiation and target materials will vary from time to time during the year, such as might be expected in the case of vegetation as it develops from the leafing stage, through growth to maturity and, finally to senescence.

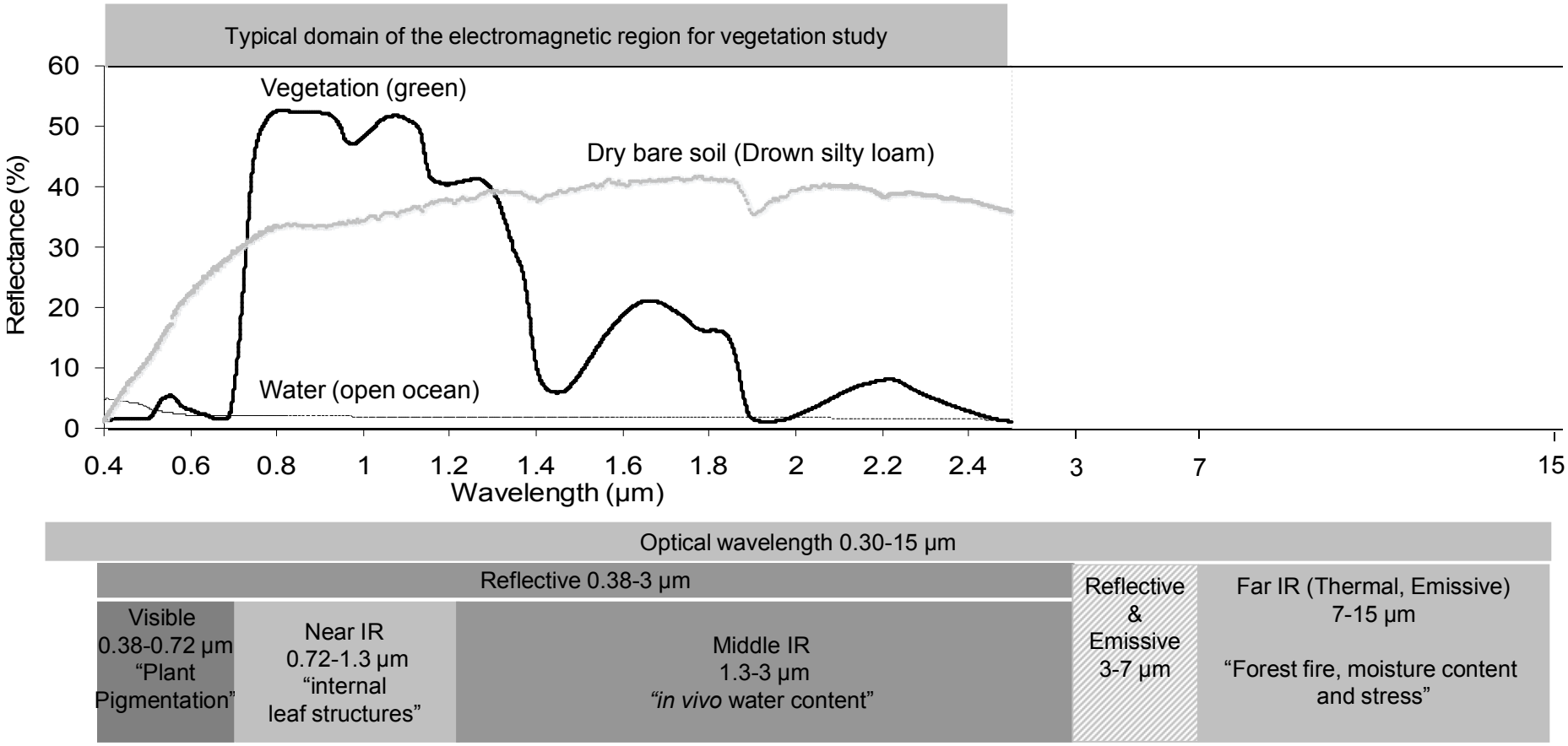

Figure 1. *Characteristic spectrum of common Earth surface materials in the visible and near to middle infrared range. The positions of the spectral domain for vegetation study, reflective and emissive optical wavelength of the electromagnetic spectrum and the fundamental control of energy-matter interactions with vegetation in this part of the spectrum are also indicated.*

Remote sensing sensors collect reflected and emitted radiation data from different parts of the electromagnetic spectrum including rarely used ultraviolet for chemical study, the most commonly used visible and infrared spectral regions followed by micro and radio waves. The visible and infrared regions, ranging from 0.30–15 μm and called "optical wavelengths", are the most commonly used spectral regions for Earth observation for both land and water surface studies (Figure 1). Optical remote sensing (optical wavelengths) uses a collection of mirrors, lenses, prisms, and other devices (placed in some specified configuration) which reflect, refract, disperse, absorb, polarize, or otherwise act on light for data collection. The optical region is generally considered to extend from 0.3/0.4–1000 μm, but it is reported in a great number of studies as a window ranging from 0.3/0.4–15 μm due to restriction by atmospheric absorption (Goetz *et al.* 1985).

Remote sensing makes it possible to collect data of inaccessible and extensive areas with information available in spectral, spatial, angular and temporal resolutions and polarization domains. Remote sensing in Earth resource analysis can be applied for physical, natural, and social sciences, e.g., geography, soil, biogeography, geology, hydrology, urban planning, agriculture, forestry, and marine sciences (Jensen 2000). Remote sensing applications in Earth resource management include monitoring deforestation in areas as big as the Amazon Basin (Rignot *et al.* 1997; Saatchi *et al.* 1997), the effects of climate change (Latifovic & Pouliot 2007; Ustin *et al.* 2009), ecosystem productivity (Crabtree *et al.* 2009), hydrology (Engman 1995), and many related environmental topics. Remote sensing also replaces costly and slow data collection on the ground, ensuring in the process that there is no interference with areas or objects. Among several application areas, remote sensing of vegetation may be the most important field of study as vegetation is a basic foundation for all living beings and small alterations can have many consequences on other living organisms and the biosphere.

Plants mediate up to 90% of the gas exchange between the terrestrial biosphere and the atmosphere (Ozanne *et al.* 2003). Minor alterations within the terrestrial carbon balance and vegetated environment can have significant impact on atmospheric carbon dioxide concentrations (Hilker *et al.* 2008) as approximately 60 gigatonnes (Gt) of carbon are annually absorbed through plant photosynthesis (Janzen 2004). Remote sensing is perhaps the only alternative way to study the status, condition, extent of vegetation and its temporal variability at multiple scales because observations can be obtained over large areas of extent with high revisitation frequency. Remote sensing of vegetation provides valuable information about the vegetation type, biophysical properties (e.g., leaf area index and biomass) and biochemical properties (e.g., chlorophyll and leaf nutrient concentration) which are used to understand ecosystem functions, vegetation growth, and nutrient cycling (Jensen & Jungho 2008). Therefore, vegetation plays a major role in global physical and biogeochemical processes and strongly regulates regional and global climate. This role is based on a simple structural unit: the leaf. The number and photosynthetic capacity of leaves in a forest control primary productivity, climate, water and carbon gas exchange, and radiation extinction and are, therefore, a key component of physiological, climatological and biogeochemical processes in ecosystems (Asner *et al.* 2003). To this regard, leaves, quantitatively determined as a leaf area index (LAI), have been extensively studied using ground based and remotely sensed optical Earth observations. LAI addresses the confounding role of vegetation as biophysical, biochemical, and radiation regime determinant parameter in our biosphere.

Optical wavelengths of remote sensing are the common electromagnetic regions used for LAI and generally for vegetation studies. This is due to the pigmentation, *in vivo* structure and moisture content of leaves which are more characteristic based on matter-specific and quantum mechanical interaction, as well as molecular structure and scattering property in optical wavelengths (Figure 1). A typical spectral curve for a healthy plant is shown in Figure 1. The leaf reflectance is controlled in the visible (0.4–0.7 μm) by the pigments in the leaves particularly chlorophyll which has high absorptance, low reflectance and transmittance in the blue and far red portion of the visible spectrum. The absorption involves electronic transitions in the chlorophyll molecule centred on the magnesium component of the photoactive site (Goetz *et al.* 1985). The blue absorption is also the effect of electronic transitions in carotenoid pigments. In the near infrared (NIR) region (0.7–1.3 μm), the dominant feature for high reflectance of leaves is associated with leaf cell structure and cellular arrangement within leaves and hydration state (Gates 1970; Slaton *et al.* 2001). The reflectance feature in the middle infrared regions (1.3–2.5 μm) is mainly dominated by the presence of water in the leaves. Generally speaking, leaf reflectance in the NIR region is affected primarily by leaf structure, whereas reflectance in the visible region (0.4–0.7 μm) is determined mostly by photosynthetic pigments, and reflectance in the middle infrared region (1.3–2.5 μm) by water content (Gates *et al.* 1965). At the transition from red to NIR wavelengths (Figure 1), leaf reflectance greatly increases, producing a distinct spectral feature referred to as the red edge. Plants consist of aggregations of leaves that form a canopy with its own scattering property which is usually addressed by LAI to describe closed canopy reflectance solutions (Suits 1973; Tucker & Garratt 1977; Verhoef 1984). On the other hand, using high contrast of reflectances in different optical wavelengths among varying amount of photosynthetic biomass and vegetated and non-vegetated surfaces, LAI, and leaf and canopy reflectances can be mathematically associated by the derivative spectral variable called spectral vegetation index (SVI) (Rouse *et al.* 1974; Tucker 1979).

A phenomenon or an object inferred from airborne or satellite remote sensing data should be calibrated and validated using the *in situ* observation (Jensen 2000). To this regard, in the past decades, several optical field instruments appeared in the literature based on the measurement of light transmission through canopies for *in situ* LAI measurements. Optical instruments such as line quantum sensors or radiometers (Pierce & Running 1988), laser point quadrats (Wilson 1963), and capacitance sensors (Vickery *et al.* 1980), canopy image analysis techniques (Digital Plant Canopy Imager CI 100, MVI), Demon (CSIRO, Canberra, Australia), the Sunfleck Ceptometer (Decagon Devices Inc., Pullman, WA, US), the most commonly used LAI-2000 Plant Canopy Analyser (LI-COR, Lincoln, Nebraska, USA), the Tracing Radiation and Architecture of Canopies (TRAC, 3rd Wave Engineering, Ontario, Canada), and hemispherical photography have been extensively used for *in situ* LAI measurements (Rich 1990; Welles 1990; LI-COR 1992; Jonckheere *et al.* 2004).

Hemispherical (fish-eye) photography, a technique that is markedly cheaper than alternatives, has already proven to be a powerful *in situ* method for measuring LAI due to numerous advances related to evolving computer, photographic, and digital technologies and scientific modelling methods (Jonckheere *et al.* 2004). Hemispherical photography is a technique to estimate solar radiation and characterize plant canopy geometry using photographs taken looking upward through an extreme wide-angle lens (Rich 1990). Spatially explicit imaging methods like hemispherical photography enable more precise corrective methods and if it is acquired with standard procedures, it can be reprocessed when improved models become available.

Nowadays, analysis of hemispherical photographs alone has been successfully used in a diverse range of studies to characterise *in situ* plant canopy structure and light penetration (Canham *et al.* 1990, Rich *et al.* 1993; Easter & Spies 1994). The LAI retrieved from airborne and satellite remote sensing following either empirical relationships between SVI and *in situ* measurements or using canopy reflectance modelling have successfully been validated using hemispherical photograph analysis (Houbork *et al.* 2009; Kuusk *et al.* 2009). As a close-range optical remote sensing method, hemispherical photography is a rapid, easy-to-use and low-cost method for canopy analysis with wide applications in forest studies, especially in forest ecological monitoring and assessment. However, LAI retrieval from close-range, airborne, and satellite observations still remains one of the most challenging research areas of the optical remote sensing of vegetation.

1.2 Leaf area index as a key biophysical parameter

A wide range of models used in agriculture, ecology, carbon cycling, climate and other studies require information on the amount of leaf material present in a given environment to correctly represent radiation, heat, momentum, water, and various gas exchanges with the overlying atmosphere or the underlying soil (Monteith & Unsworth 1990). LAI thus often features as a critical state variable in these models to represent the interaction between vegetation surface and the atmosphere, e.g. radiation uptake, precipitation interception, energy conversion, momentum and gas exchange, as all areas are substantially determined by the vegetation surface. During the growing season of deciduous trees, the total vegetation surface itself is mainly composed of leaf area, and by a lesser part of twigs, branches and stem surface. Fournier *et al.* (1996) suggested that branches and boles contributed to total LAI by less than 5% in three relatively dense stands of conifers.

LAI represents the amount of leaf material in ecosystems and controls the links between biosphere and atmosphere through various processes such as photosynthesis, respiration, transpiration and rain and radiation interceptions. Therefore, LAI is fundamentally important as a parameter in land-surface processes and parameterizations in global and regional climate models and biosphere/atmosphere exchange of carbon dioxide, water vapour and energy (Scurlock *et al.* 2001).

LAI is largely used in agro-meteorology, nevertheless many atmospheric circulation or biogeochemical models rely on it to parameterize the vegetation cover, or its interactions with the atmosphere. For instance, evapotranspiration and carbon fluxes between the biosphere and the atmosphere are routinely expressed in terms of the LAI of the canopy (Gobron & Verstraete 2008). Consequently, LAI appears as a key variable in many models describing biosphere-atmosphere interactions, particularly with respect to the carbon and water cycles (GCOS 2004). Currently, LAI is set as an "essential climate variable" by Global Terrestrial Observing System (GTOS), Food and Agriculture Organization of the United Nations (FAO), and Global Climate Observing System (CCOS) (GCOS 2004 & 2008; Gobron & Verstraete 2008). LAI is, for example a standard parameter observed at all FLUXNET sites.

Various national and international projects, like the GLOBCARBON project funded by European Space Agency (ESA), Moderate Resolution Imaging Spectroradiometer (MODIS) and Multiangle Imaging SpectroRadiometer (MISR) products funded by National Aeronautics and Space Administration (NASA), the CYCLOPES (Cycle and Change in Land Observational Products from an Ensemble of Satellites) product operating within the framework of the POSTEL (Pôle

d'Observation des Surfaces continentales par TELédétection) Thematic Centre, and Land Surface Analysis Satellite Applications Facility (LSA SAF) products derived from the Meteosat families of satellites (MSG and EPS) of EUMETSAT, to name but a few, provide regional and global level estimates of LAI and other land surface parameters. The validation exercises are performed in the framework of ground based networks, including both national research groups and international entities, such as the Land Product Validation (LPV) Subgroup of the CEOS Working Group on Calibration and Validation (CEOS-WGCV).

LAI is applied as a single determinant parameter for various studies. For example in earlier days, LAI was used as a sole indicator for radiation interception and availability with crop growth rate (Stern & Donald 1961). Values of LAI are used for scaling between leaf-level measurements of water vapour and CO_2 conductance and flux, and estimates of these conductance and fluxes for the total vegetation–atmosphere interface (McWilliam *et al.* 1993). Waring (1983) used LAI of forests as an index of growth and canopy light competition. The successful implementation of the role of vegetation in climate modelling requires plausible specification of the numerical parameters needed by the underlying theory. To this regard, Buermann *et al.* (2001) used satellite-based LAI data in improving the simulation of near-surface climate in the NCAR CCM3 (National Center for Atmospheric Research Community Climate Model) global climate model. Land surface evapotranspiration constitutes evaporation from wet leaf surfaces, transpiration from leaves, and evaporation from the soil. The wetness of leaves, which is the interception storage capacity is a direct function of leaf area index. To this regard, LAI have been used for estimating catchment evaporation and runoff (Zhang *et al.* 2008), and on seasonality assessment of the annual land surface evaporation in a global circulation model (Hurk *et al.* 2003). Therefore, monitoring the distribution and changes of LAI is a vital means for assessing growth and vigour of vegetation on the planet and accurately representing the ecosystem functioning.

1.3 Definition of leaf area index

LAI as a major deriving factor in soil-vegetation-atmosphere, biogeochemical cycles, and agro-meteorology models often require long time series measurements, and therefore consistent definition at various temporal and spatial scales. During past decades, various definitions of LAI have been provided by scientists from many disciplines for a range of purposes. A definition of LAI needs to be precisely addressed to make research results comparable. Regrettably, many individual reports of LAI in the literature fail to provide details of the LAI definition assumed. Here, I categorised the definition of LAI into three broad groups based on: (a) the assumptions of leaf shapes, (b) the purpose of measurements, and (c) the different correction levels applied to get final true and green LAI.

LAI was first defined by Watson (1947) as the total one-sided area of photosynthetic tissue per unit ground surface area. The term ‘one-sided’ is not straight forward as the shape of leaves or other photosynthetic plant organs can vary from needles, succulent photosynthetic tissues, and broadleaves to Bryophytes. In the original definition by Watson (1947), leaves were assumed to be flat with zero thickness. The simplest description of LAI is:

$$LAI = L / A \quad (1)$$

L is the leaf area of a canopy per unit ground surface area *A*. Traditionally, *L* is measured as a projected area after placing leaves on a horizontal surface in order to avoid shape dependency of LAI (Chen & Black 1992) and to use the common value of 0.5 as an average projection coefficient (G), which is common for optical derivation of LAI when the leaf angle distribution is spherical (random). Parameter *G* is the mean ratio of projected to one-sided leaf area, where 'projected leaf area' refers to the sum of the shadow areas cast by leaves on a plane perpendicular to the beam direction (Stenberg 2006). The above definitions and assumptions cannot be applied as such to non-flat leaves. Table 1 summarises the violation of the assumption that the projected surface is half of the total leaf surface area. This can be described in the following example. A disk and a sphere with the same diameter have the same maximum projected area, but the sphere intercepts twice as much light as the disk with random angular distribution when averaged for all radiation incidence angles. This means that half the surface area of a sphere is twice the area of half the surface area of a disk. Since the leaves can be oriented in all directions, the projected area in one direction does not carry all the necessary information. To this end, Chen & Black (1992) suggested that the LAI of non-flat leaves be defined as half the total intercepting area per unit ground surface area and that the definition of *L* based on the projected leaf area be abandoned. The relationships between projected area and total or half surface area of leaves are shape specific (Table 1).

Table 1. *Leaf shape and area (L is projected leaf surface area, ≈ is approximately equal to). Sources: Chen & Black 1992; Chen & Cihlar 1996; Barclay 1998; Asner et al. 2003.*

Leaf shape	Total surface area	Half the total surface area	Example
Flat	2L	≈ L assuming infinitively thin leaves	Broadleaves
Needle	>2L	≈ 1.28L for circular cylinders representing conifer needles, and ≈ 2L for spheres or square bars representing highly clumped shoots and some spruce needles	Conifers
Photosynthetic stem	>2L	≈ 1.57L representing cylindrical green branches	Cactus
Succulent leaves	2L to >2L	≈ L to ≈ 2L	Aloe
Bryophytes		Varies	Non-vascular plants, mosses, liverworts
Litter/dead foliage		Varies (refer above)	All leaf types

Barclay (1998) and Barclay & Goodman (1998) discussed that at least five common measures of LAI exist based on the different purposes for which LAI is determined (e.g. vegetation growth, physiological activity, light attenuation). The most accepted ones are summarised in Table 2, including the most common definition in recent studies. The 'total LAI' definition used to be the common measure in earlier studies for coniferous needle areas (P. Stenberg, personal communication, 2009) and currently rarely employed. Most published values of LAI utilize 'one-sided' and 'horizontally projected' LAI definitions (Table 2). 'One-sided' LAI definition lacks the meaning of 'one-sided' for non-flat, highly clumped, or rolled leaves. Chen & Black (1992) suggested abandoning 'horizontally projected' LAI definition because it has neither physical nor biological significance. Barclay (1998) concluded that most

***Table 2**. Common measures of LAI.*

Term	Definition	Description and purpose	Method	References
Total LAI	The total surface area of the leaves, taking leaf shape into account per unit ground surface area below the canopy	Currently, rarely employed. Used for ecophysiological studies such as gas exchange, radiation interception and stomatal conductance particularly in conifer forests. Diffuse light makes up a larger proportion of total irradiance at low sun angles and under cloudy conditions. Confer forests are prevalent in high latitude, where sun angles are low and in temperate rain forest, where conditions are usually cloudy. Therefore, total LAI is mainly used in conifer forests because conifer needles absorb more diffuse light per unit projected leaf area than flat leaves	Direct harvesting, allometry	Kozlowski & Schumacher 1943; Cable 1958; Madgwick 1964
One-sided LAI	One-sided leaf area per unit ground surface area assuming that leaves are flat with zero thickness, even if the leaves are not planar	The meaning of 'one- sided' is unclear for coniferous needles, highly clumped foliage or rolled leaves	By specific leaf area relationship, destructive harvesting, using square grid paper, allometry	Watson 1947
Horizontally projected LAI	The area of 'shadow' that would be cast by each leaf in the canopy with a light source at infinite distance and perpendicular to it, summed up for all leaves in the canopy	Common in remote sensing applications because it represents the maximum leaf area that could be seen by sensors from overhead	Plumb lines, inclined point quadrats, using square grid paper, optical field instruments, Ceptometers, allometry	Grace 1987; Ross 1981
Hemi-surface LAI	One half the total leaf surface area per unit ground surface area projected on the local horizontal datum	The main difference with 'one-sided LAI' definition is that the one-side in 'hemi-surface LAI' is explicitly expressed as half the total surface area of the leaves and the LAI is referred to horizontal local datum which makes the estimate independent of local slope. Used for modelling photosynthesis, transpiration, light interception, albedo, precipitation interception, canopy microclimate, radiation extinction, and water, carbon, and energy exchange with the atmosphere	Optical ground and remote sensing measurements, allometry	Lang *et al.* 1991; Chen & Black 1992; Loveland *et al.* 1998; Walter & Torquebiau 2000

of the definitions of LAI in the literature have no predictable relationship with each other. However, contradictory to the conclusion of Barclay (1998), Johnson (1984) in earlier study demonstrated good convergence between the projected and total surface area of Pinus needles. This study is overlooked by the scientific community. Recently, the most widely accepted LAI definition is the 'hemi-surface LAI', i.e., one half the total leaf surface area per unit ground surface area projected on the local horizontal datum. This indicates that the measure of LAI is independent of local slope (Loveland *et al.* 1998; Walter & Torquebiau 2000; Fernandes *et al.* 2004). This manuscript assumes the 'hemi-surface LAI' definition (Table 2).

Many optical field instruments measure canopy gap fraction based on radiation transmission through the canopy. The LAI measures from these instruments based on the gap fraction are problematic due to the complexity of canopy architecture in natural forest stands. Therefore much effort and correction steps are needed to improve these techniques. The direct output of many optical field instruments is 'effective LAI' or 'effective plant area index' by assuming that foliage elements (including branches, stems, leaves, flowers and cones) are spatially randomly distributed. The final true and green LAI may only be measured using a planimeter using all possible allometric relationships in order to reduce the sampling (Frazer *et al.* 1997). Since LAI using optical field instruments is usually measured near the ground surface based on radiation transmission, all aboveground materials, including green and dead leaves, branches, and tree trunks and their attachments (lichen, moss), intercepts light and are included in LAI. In addition to this, in the forest growing in sloping ground, LAI measurements are affected by ground slope (Walter & Torquebiau 2000). Therefore, for the ground based optical LAI measurements, there are several indispensable steps for the correction of obtained LAI. Table 3 presents the different correction stages and definition of LAI at each stage.

Table 3. *Common measures of LAI based on different correction stages.*

Term	Definition	References
Effective leaf area index or effective plant area index	One half the total leaf surface area per unit ground surface area based on the assumption that foliage elements (including branches, stems, leaves, flowers and cones) are randomly distributed in space. Effective LAI describes the radiation interception and radiation regime within and under canopy	Black *et al.* 1991; Chen *et al.* 1991
True leaf area index or true plant area index	One half the total leaf surface area per unit ground surface area after correcting for canopy non-randomness. True LAI is corrected for the spatial distribution pattern of foliage elements (including branches, stems, leaves, flowers and cones)	Nilson 1971
Green leaf area index	One half the total green leaf surface area per unit ground surface area. By removing the contributions of non-leafy materials by assuming they have a spatial distribution pattern similar to that of leaves	Chen *et al.* 1997
Green leaf area index corrected for topographic slope	One half the total green leaf surface area per unit ground surface area projected on the local horizontal datum. LAI is corrected for slope and referred to the horizontal surface	Fernandes *et al.* 2004

Most of the definitions of LAI presented in Table 1–3 are mainly linked to ground based optical measurements of LAI. Airborne or satellite based estimation of LAI is an indirect approach, relying on the relationship between LAI and the characteristics of the solar radiation reflected from the canopy, as measured by optical

sensors. The definition of LAI used in satellite or airborne remote sensing is rather linked to the state variable corresponding to the canopy optical depth measured along the vertical. The ground based optical measurements give the "plant area index" which includes non-photosynthetic parts of plants as shown above. On the other hand, the LAI retrieved from satellite or airborne remote sensing refers to the "greenness index" including the understorey by looking at the canopy from above, which is highly relevant from an application and vegetation function point of view for photosynthesis, evapotranspiration and carbon balance studies. This definition variation between ground based and remotely obtained LAI measurements is usually ignored in the literature.

1.4 Aim and structure of the dissertation

The main purpose of this dissertation is to enhance the determination of LAI using close-range remote sensing (hemispherical photography), airborne remote sensing (high resolution colour and colour infrared imagery), and satellite remote sensing (high resolution SPOT 5 HRG imagery) (Figure 2). The commonly used light extinction models are applied at all levels of optical observations. For the sake of comparison analysis, LAI is further determined using statistical relationships between spectral vegetation index (SVI) and ground based LAI. To achieve these, the following specific objectives were targeted:

- Section 1 and 2 comprises detailed literature review about optical remote sensing of LAI and its definitions,
- The second part of the dissertation focuses on the enhanced determination of LAI using hemispherical photography particularly sampling of gap fraction dataset (I), slope corrections applied for LAI (II), and clumping index computations (III),
- The third part of the dissertation focuses on the spectral sensitivity of SVIs to LAI (IV), and
- The last part is dedicated to the feasibility of applying the same light extinction models used for hemispherical photography in the first three papers in airborne (V; VI) and satellite datasets (VII) for large scale LAI determinations.

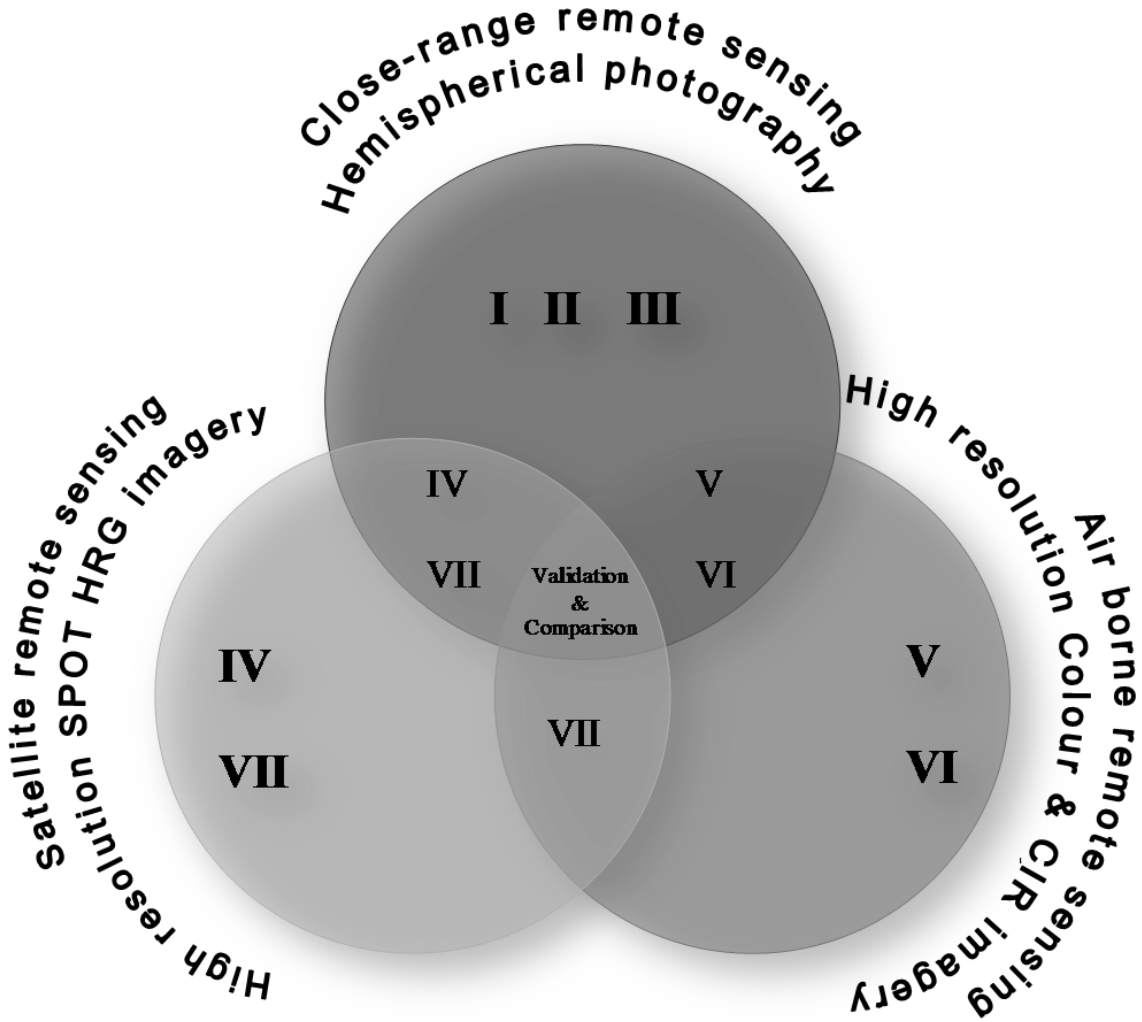

Figure 2. *Summary of the remote sensing data and the conceptual locations of the leaf area index retrieval approaches examined in Papers I–VII.*

2. OPTICAL REMOTE SENSING OF LEAF AREA INDEX

Several direct and indirect methods for estimating LAI have appeared in the literature (Ross 1981; Campbell & Norman 1989; Norman & Campbell 1989; Welles 1990; Bréda 2003; Jonckheere *et al.* 2004). All direct techniques for estimating LAI are very labour intensive, including harvest (Dufrêne & Bréda 1995), point quadrat (Warren-Wilson 1959), allometric and litter-collection methods (Waring *et al.* 1982). Direct methods, although accurate, are not feasible in many locations and extensive areas, and they are very time-consuming compared to optical estimates. Allometric equations from different geographic locations should be used with caution due to the influences of tree size, species, and edaphic conditions. Chen (1996) has indicated that optical methods can provide even more reliable LAI estimates than destructive sampling techniques. Indirect methods, that relate leaf area to the radiation environment, are generally less time-consuming and consequently received a great deal of thought in both theory and instrumentation. Several remote sensing methods and ground based optical instruments (see section 1.1.; Welles 1990; Bréda 2003; Jonckheere *et al.* 2004) estimate LAI indirectly by measuring light transmission, gap fraction, and canopy reflectances using theoretical light extinction models (Nilson 1971; Lang & Xiang 1986; Perry *et al.* 1988; Campbell & Norman 1989; Norman & Campbell 1989). The following sections describe the most widely used light extinction models and approaches for LAI determination using both close-range and remotely sensed optical observations.

2.1 Ground based optical determination of leaf area index

Ground based optical determination of LAI is usually based on the measurements of the transmission of radiation through the canopy, making use of the radiative transfer theory (Anderson 1971; Ross 1981). These methods are non-destructive and are based on a statistical and probabilistic approach to foliage elements (or its complement, gap fraction) distribution and arrangement in the canopy (Jones 1992). There are generally three types of ground based optical measurements of LAI (Wulder & Franklin 2003): (a) measuring diffuse light transmission or record canopy gaps within a hemispherical view (e.g., LAI-2000 and hemispherical photography), (b) measuring the direct solar irradiance (sunflecks) at a known solar angles along a transect (e.g., DEMON, quantum sensors, and TRAC), and (c) measuring the vertical distribution of canopy elements (optical point-quadrant method). All the aforementioned radiation measurement and gap fraction based methods commonly use related light extinction models to describe the canopy structural variables. In recent years, among several ground based optical instruments, hemispherical photography is becoming the most commonly used method because of the advances in digital photography, image analysis, and data processing.

Interception of radiation by plant canopies is described in many physiological models using Beer's law (Monteith & Unsworth 1990; Jones 1992). A common feature of the gap proportion formulae used for LAI determination indicates that the logarithm of the gap proportion is a linear function of the downward cumulative LAI expressed generally as:

$$P_{\theta,\varphi} = \exp(-kLAI) \quad (2)$$

where P is a gap fraction (a probability of non-interception) for a direction defined by zenith θ and azimuth φ angles and k is an extinction coefficient. k is a function of leaf optical properties and the geometry of the leaf relative to the beam of light penetrating the canopy (Campbell 1986). Values of k can be calculated by approximating the distribution of leaves within a canopy to that of the surface area of spheres, cylinders or cones (Monteith & Unsworth 1990). The existing theoretical models explain the various ways of addressing the values of k. Nilson (1971) gives a theoretical description of the most commonly used light extinction models. Based on the assumption of foliage distributions, Nilson (1971) categorised the light extinction models into three classes: (a) Poisson model, (b) Markov model, and (c) binomial model (positive and negative) (Table 4).

Table 4. *Theoretical light extinction models with their assumptions and equation for LAI determination. Significant improvement is introduced after Nilson (1971) by adopting the models for non-flat terrain (II).* ***Where*** *P is the probability of non-interception or gap fraction for a direction defined by zenith* θ *and azimuth* φ *angles, LAI is the leaf area index,* Ω *is the Markov parameter (clumping index), N is equal and statistically independent layers, g is the independent layer thickness or the binomial clumping index which can be retrieved for each stand if LAI and N are known,* $\cos\gamma$ *is a correction factor for path length (II),* $\cos\beta$ *is a correction factor of gap fraction for ground slope* β*, and* $G_{\theta,\varphi}$ *is the mean projection of a unit leaf area in the direction of the beam and onto a plane normal to the beam. When* β *= 0,* $\cos\beta$ *is 1 and* $\cos\gamma = \cos\theta$*, therefore all the equations are the same with the light extinction models described in Nilson (1971).*

Model	Expression of LAI regarding to the non-interception or gap fraction	Assumptions of foliage elements distribution within a canopy
Poisson model	$LAI = -\frac{\ln P_{\theta,\varphi}\cos_{\gamma}}{G_{\theta,\varphi}\cos_{\beta}}$ (3)	Random foliage dispersion. The stand consists of a very large infinite number of statistically independent horizontal layers, N. The probability of observing more than one contact per layer is infinitely small compared with the probability of observing one contact (leaves do not overlap within a layer). The probability of observing a contact within a layer is equal to the mean number of contacts per layer.
Markov model	$LAI = -\frac{\ln P_{\theta,\varphi}\cos_{\gamma}}{\Omega_{\theta,\varphi}G_{\theta,\varphi}\cos_{\beta}}$ (4)	Regular and clumped foliage dispersion. The probability of a contact in a horizontal layer depends on whether there has been a contact in the previous layer (Markov property).
Positive binomial model	$LAI = \frac{\ln P_{\theta,\varphi}g}{\ln\left[1-g(G_{\theta,\varphi}/\cos_{\gamma})\right]}/\cos_{\beta}$ (5)	The stand consists of a finite number of equal and statistically independent layers, N. Regular dispersion of foliage.
Negative binomial model	$LAI = -\frac{\ln P_{\theta,\varphi}g}{\ln\left[1+g(G_{\theta,\varphi}/\cos_{\gamma})\right]}/\cos_{\beta}$ (6)	The stand consists of a finite number of equal and statistically independent layers, N. Clumped dispersion of foliage.

Both positive and negative binomial models may be used when the canopy can be divided into a finite number of equal and statistically independent layers and

require an additional parameter ΔL, representing the thickness of each layer. Binomial models tend toward the Poisson as the number of layers N increases ($N \to \infty$) and the thickness ΔL decreases$\to 0$. Positive binomial model may also describe a random dispersion with independent layers (T. Nilson, personal communication, 2009). However, based on the standard statistical indicators for dispersion measurements such as relative variance of contact numbers, positive binomial model describes more regular than Poisson distribution. Therefore, for the dependent layers, alternative approaches such as Markov chain models are being used. Nilson (1999), and later improved by Nilson & Kuusk (2004), proposed a new algorithm for LAI estimation. However, due to the requirements for additional stand variables (stand density, tree height, crown depth, canopy closure, crown closure, shoot-level clumping index, and branch/leaf area ratio) other than gap fraction, this algorithm is generally overlooked. The existing theoretical models explain the various ways of addressing the values of k particularly for the most widely used Poisson model. The major ones can be grouped according to approaches by Miller (1967), Lang (1986, 1987) and Campbell (1990).

Miller approach

From gap fraction analysis, Miller's integral can be estimated over 0 to $\pi/2$ as follows (Miller 1967):

$$LAI = -2\int_0^{\pi/2} \ln P_\theta \cos\theta \sin\theta d\theta \quad (7)$$

As most gap fraction data are retrieved over a limited zenith view angle ranges often $<\pi/2$, the following equation can be used for the approximation of Miller integral:

$$LAI = -2\frac{\sum_{i=1}^{n} \ln P_{\theta_i} \cos_{\theta_i} \sin_{\theta i} d\theta_i}{\sum_{i=1}^{n} \sin_{\theta i} d\theta_i} \quad (8)$$

where n is the number of zenith angles being used. The formula uses a $\sin_{\theta_i} d\theta_i$ weighting, normalized to the sum of 1 for each angle-dependent estimation of LAI, between the limits of the integral. This property, among other considerations, allows the calculation over a more restricted zenith angle range. For example, calculation may be applied over 55°–60° of zenith angle. This range of angles is useful as the sun's beam incidence angle θ_b = 57.3 (≈ 1 radian), where the mean projection of leaf area G_θ and the extinction coefficient k_θ are virtually independent of the leaf angle distribution.

Lang approach

From equation (3), the following expression can be derived:

$$-\cos_\theta \ln P_\theta = LAIG_\theta = K_\theta \quad (9)$$

where K_θ is the mean contact number. The mean contact number is determined by the overlapping of projected areas of leaves on a plane perpendicular to the direction of the ray of light, which penetrates the canopy along a given path length. Lang (1986) argued that LAI and average leaf inclination angle (ALIA) may be recovered from the inversion of equation (9), using the relationship:

$$K_\theta = a + b\theta \quad (10)$$

where a is the intercept and b is the slope of the regression of $-\cos_\theta \ln P_\theta$ (K_θ) against θ in radians. Using the original Miller's integral for flat leaves with symmetry about azimuth yields:

$$LAI = 2\int_0^{\pi/2} K_\theta \sin\theta d\theta \quad (11)$$

By substituting (10) into (11):

$$LAI = 2(a+b) \quad (12)$$

Equation (12) is the exact solution to Miller's integral. This simple equation yields the effective LAI (Section 1.3). An estimate of ALIA can be calculated from *b*, the slope of the regression of K_θ against θ using a sixth order polynomial (Lang 1986). A great advantage of this approach is the possibility to estimate the statistical reliability of LAI and ALIA, derived from the goodness-of-fit of the regression.

Campbell approach

Campbell method relies on the ellipsoidal distribution function of leaf angles (Campbell 1990). The ellipsoidal distribution function assumes that the leaf angles in the canopy are "distributed like the angles of normals to small area elements on the surface of an ellipsoid". Using this approach, equation (2) can be rewritten as:

$$-\ln P_\theta = LAIk_\theta \quad (13)$$

where k_θ is the extinction coefficient for zenith angle θ averaged overall leaf angles and defined as:

$$k_\theta = \frac{\sqrt{x^2 + \tan^2\theta}}{x + 1.774(x+1.182)^{-0.733}} \quad (14)$$

The 'shape parameter' x may be defined as the ratio of vertical to horizontal foliage area projections, which describes the shape of the distribution. For example, if $x = 1$, leaves have a spherical distribution. The canopy tends to be 'horizontal' or planophile, when $x > 1$ and 'vertical' or erectophile, when $x < 1$. The shape parameter determines an ellipsoidal extinction coefficient k_θ and a normalized ellipse area. A non-linear constrained least-squares technique finds values of x and LAI. ALIA can be derived as a function of x (Norman & Campbell 1989):

$$ALIA = 90(0.1 + 0.9\exp(-0.5x)) \quad (15)$$

So far, the common methods used to estimate canopy structural information from gap fraction measurements has been limited to a discussion of canopies with randomly distributed foliage elements that can be modelled using a Poisson distribution (van Gardingen *et al.* 1999). To allow the use of the Poisson law, the concept of effective LAI is introduced (Section 1.3; Chen & Black 1991), which corresponds to the product of a clumping index with the true LAI estimate. In natural canopies, foliage clumping occurs mostly at the shoot level for conifer trees, but may also occur at the branch and crown levels for most forest types. Conventional LAI estimation techniques normally lead to significant underestimates of the LAI (Chen *et al.* 1991; Smith *et al.* 1993) when the analysis assumes a Poisson distribution, though Whitford *et al.* (1995) reports large overestimates. Despite the challenges, there have been significant efforts to calculate clumping index from multi-look angle gap fraction datasets such as hemispherical photography based on varying gap fraction averaging methods and gap size distribution theories (summary: Walter *et al.* 2003; Leblanc *et al.* 2005; III).

Ground based optical leaf area index determination in non-random canopies

Foliage elements can be distributed in a space in random, clumped or regular dispersions. If the foliage dispersion is non-random, Poisson model for LAI estimation either underestimates in the case of clumped, or overestimates in the case of regular foliage distribution. The regular (geometric) distribution can be expressed with positive binomial distribution, whereas clumped distribution can be expressed with negative binomial distribution (Nilson 1971). As aforementioned, binomial distribution function is not feasible for gap fractions measured using optical field instruments. The other approach particularly applied for gap fraction measurements from LAI-2000 was to calibrate gap fraction estimates with independent LAI estimates (e.g., Chason *et al.* 1991; Stenberg *et al.* 1994; Stenberg 1996a; Cherry *et al.* 1998; Barclay & Trofymow 2000; Nackaerts *et al.* 2000). Geometric relationships describing foliage distribution on branches can also be used to derive correction factors (Chen & Black 1992; Stenberg *et al.* 1994; Stenberg 1996b; Fournier *et al.* 1997). However, these approaches are empirical and not universally applicable as the gap fraction and independent LAI estimates relationship varies between species and between stands of the same species. All of these techniques can be considered to work by correcting the extinction coefficient which is reduced in clumped canopies and increases in regular canopies.

Generally speaking, clumping increases the canopy gap fraction for a given LAI. In theory, Lang & Xiang (1986) suggested a procedure to estimate LAI for discontinuous canopies using a spatial logarithmic averaging of sunbeam fractional measurement:

$$\Omega_{LX} = \frac{\ln \overline{P_{\theta,\varphi}}}{\overline{\ln P_{\theta,\varphi}}} \quad (16)$$

where values of the probability of non-interception (gap fraction, P) are averaged as $\ln \overline{P_{\theta,\varphi}}$ where $\overline{P_{\theta,\varphi}}$ are localised P values linearly averaged over a fixed distance defined relative to the characteristic width of a leaf, assuming Poisson distribution at

this scale. The choice of length-scale for logarithmic averaging is influenced by two considerations: (a) the Poisson distribution is strictly only valid for an infinite number of foliage elements, and (b) the probability of obtaining a gap fraction of zero increases as the length-scale decreases. As the logarithm of zero is undefined, this approach will perform poorly as the length scale approaches the limit defined by the average width of individual foliage elements (van Gardingen 1999). Another modification of this was to calculate an average LAI from local azimuthal values (Walter *et al.* 2003). Both logarithmic averaging and azimtuhal averaging of local estimates constitute 'quasi-random' methods (Planchais & Pontailler 1999).

Neumann *et al.* (1989) presented a unique method based on the spatial autocorrelation of gap fractions to retrieve clumping index. The clumping index was calculated from conditional probability of a light ray passing through the canopy in the same opening separated by a Δd. However, this method was not thoroughly evaluated as the choice of Δd influences the computed conditional probability. More advanced clumping index calculation is based on the Chen & Cihlar (1995) gap size distribution theory developed for TRAC instrument. As clumped canopies are characterised by large gaps intermingled with small gaps, Leblanc (2002) later modified by Leblanc *et al.* (2005) formulated the derivation of clumping index as:

$$\Omega_{CC} = \frac{\ln[F_m(0,\theta)]}{\ln[F_{mr}(0,\theta)]} \frac{[1-F_{mr}(0,\theta)]}{[1-F_m(0,\theta)]} \quad (17)$$

where $F_m(0,\theta)$ is the measured accumulated gap fraction larger than zero, i.e., the canopy gap fraction, and $F_{mr}(0,\theta)$ is the gap fraction for the canopy when large gaps that are theoretically not possible in a random canopy have been iteratively removed for a given LAI and foliage element width. This method takes the advantages of both the gap fraction and the gap size information, which can be applied to all types of plant canopies without the need for spatial pattern assumptions about canopy elements unlike logarithmic gap fraction averaging methods. The relatively recent advancement in gap size based theory is the segregation coefficient developed by Pielou (1962) and adapted to gap size data obtained from hemispherical photography by Walter *et al.* (2003). This method is based on the probability of encountering sequences of gap and foliage pixels on hemispherical photograph. The only difference between Chen & Cihlar (1995) and Walter *et al.* (2003) clumping index methods is that the first is based on a gap size accumulation (Equation 17), whereas the second relies on a gap size distribution. The inherent problem associated with gap size based approaches is the heterogeneity of the gap size within the segments, whereas with gap averaging method the result is influenced by the segment size. To this regard, Leblanc *et al.* (2005) proposed, the combination of gap size and logarithmic averaging methods and proven later to be robust approach (III).

Despite all these studies, foliage clumping remains as one of the challenging issues of remote sensing of LAI. It is perhaps surprising to discover that clumping index methodologies are not the centre of research attention. For example, logarithmic gap averaging methods suffer from lack of knowledge for how the gap fraction sampling size is practically defined (I). In addition to this, the majority of world forests occur in heterogeneous ecosystems and topography with rather complex canopy architecture. Therefore, the LAI estimation from gap fraction is not only affected by the foliage aggregation on space but also by the local topography such as ground slope (II; III). This indicates that there are still a great deal of improvements for the ground based optical determination of LAI from *1D* or *2D* gap fractional

measurements (I–III). The accuracy with which the ground based LAI measurements are acquired and determined is an indispensable step for both calibration and validation of LAI retrievals from airborne or satellite optical remote measurements.

2.2 Empirical modelling of leaf area index

A number of mathematical formulas using mainly visible and near infrared reflectances, here called spectral vegetation indices (SVI), have been proposed for relating ground, airborne or satellite radiometric measurements to the amount of vegetation presence (Table 5). This argument was strongly supported even in relatively earlier studies as leaf reflectance measurements of visible and near infrared energy identified a strong correlation between a red and near infrared transmittance ratio and measured LAI (Jordan 1969). Even though new SVIs are still being developed, Perry & Lautenschlager (1984) discussed 20 SVIs many years ago, and the formal relationships among them. It should be noted also that, normalized difference vegetation index (NDVI) still remains the most widely used SVI to this date. SVIs were designed to maximize sensitivity to the vegetation's characteristics or optical thickness while minimizing confounding factors such as soil background reflectance, directional, topographic, and atmospheric effects. Coppin & Bauer (1994) concluded that vegetation indices can be grouped into three major categories: namely, 'brightness', 'greenness' and 'wetness'. Relatively recently, Brown *et al.* (2000) recommended that inclusion of shortwave infrared (SWIR) reflectance in SVIs may be useful to suppress the background soil or land cover variation influences for empirical LAI modelling.

The basic assumptions for the formulation of SVIs are: algebraic combination of remotely sensed spectral bands can be related with the amount of photosynthetic biomass and all bare soil form a line in spectral space. These are strongly supported by experimental results. Most of SVIs are constructed using NIR and red spectral space so that forming NIR-red line for bare soils (zero vegetation). Based on the diverging lines relative to the soil line, all SVIs listed in Table 5 can be categorised into two classes: (a) ratio indices which measure the slope of the line between the point of convergence and the NIR-red point of the pixel (e.g., NDVI, SAVI, SR), and (b) perpendicular/orthogonal indices which measure the perpendicular distance for the soil line to NIR-red point of the pixel (e.g., PVI, WDVI, DVI). In ratio based indices, all equal vegetation (isovegetation) lines converge at a single point, whereas in perpendicular indices the lines remain parallel to the soil line.

There have been several statistical approaches to empirically retrieve LAI based on the relationship with SVI. Most studies use least square regression (LSR) analysis spanning from linear to exponential to polynomial (e.g., Chen & Cihlar 1996; Chen *et al.* 2002). Based on LSR analysis, studies have produced large scale regional LAI map (e.g., Canada wide LAI product: Chen & Cihlar 1996; Brown *et al.* 2000; Chen *et al.* 2002). Not often used but satisfactory results were also obtained using nonparametric regression analysis such as the neural network (Liang *et al.* 2003; Liang & Fang 2004), the projection pursuit regression (Liang & Fang 2004), and Thiel-Sen regression (Fernandes *et al.* 2003). The obvious limitation of LSR is that it implicitly assumes an underlying normal structural data model to arrive at unbiased estimates. Besides, LSR regression assumes that the errors are (spatially) independent and that there are no measurement errors in the independent (SVI) variable. Therefore, in the presence of measurement errors when the regression problem is based on a functional rather than structural data model, LSR can be a biased predictor.

Table 5. *List, functional purpose and example application of the most widely used spectral vegetation indices (SVI) for leaf area index (LAI) retrieval.*

SVI	Formula	Purpose	Source	References in LAI estimation
Simple ratio (SR)	ρ_{NIR} / ρ_R (18)	Basic index	Jordan 1969	North 2002; Soudani *et al.* 2006
Normalized difference vegetation index (NDVI)	$(\rho_{NIR} - \rho_R)/(\rho_{NIR} + \rho_R)$ (19)	Basic index	Rouse *et al.* 1974	North 2002; Stenberg *et al.* 2004; Soudani *et al.* 2006 ; Stenberg *et al.* 2008
Difference vegetation index (DVI)	$\rho_{NIR} - \rho_R$ (20)	Basic index	Tucker 1979	Sasaki *et al.* 2008
Soil adjusted vegetation index (SAVI)	$(1+L)(\rho_{NIR} - \rho_R)/(\rho_{NIR} + \rho_R + L)$ (21)	Index that minimise soil noise	Huete 1988	Elvidge & Zhikang 1995; North 2002; Soudani *et al.* 2006 ; Sasaki *et al.* 2008
Transformed soil adjusted vegetation index (TSAVI)	$\left[a(\rho_{NIR} - a\rho_R - b)\right]/\left[a\rho_{NIR} + \rho_R - ab\right]$ (22)	Index that minimise soil noise	Baret *et al.* 1989	Rondeaux *et al.* 1996
Modified soil adjusted Vegetation index (MSAVI)	$\left[2\rho_{NIR} + 1 - \sqrt{(2\rho_{NIR}+1)^2 - 8(\rho_{NIR} - \rho_R)}\right]/2$ (23)	Index that minimise soil noise	Qi *et al.* 1994	Rondeaux *et al.* 1996 ; North 2002; Haboudane *et al.* 2004
Perpendicular vegetation index (PVI)	$\left[\rho_{NIR} - a\rho_R - b\right]/\left[\sqrt{a^2+1}\right]$ (24)	Index that minimise soil noise	Richardson & Wiegand 1977	Elvidge & Zhikang 1995
Weighted difference vegetation index (WDVI)	$\rho_{NIR} - a\rho_R$ (25)	Index that minimize soil noise	Clevers 1989	North 2002
Atmospherically resistant vegetation index (ARVI)	$\frac{\rho_{NIR} - \rho_{RB}}{\rho_{NIR} + \rho_{RB}}, where\ \rho_{RB} = \rho_R - \Psi(\rho_R - \rho_B)$ (26)	Index that minimise atmospheric noise	Kaufman & Tanre 1992	Rondeaux *et al.* 1996 ; Soudani *et al.* 2006
Infrared simple ratio (ISR)	ρ_{NIR} / ρ_{SWIR} (27)	Index that minimise atmospheric noise	Fernandes *et al.* 2003	Fernandes *et al.* 2004; Stenberg *et al.* 2008
Modified simple ratio (MSR)	$\left[\rho_{NIR} / \rho_R - 1\right]/\left[\sqrt{\rho_{NIR} + \rho_R} + 1\right]$ (28)	Index that can be linearly related to LAI	Chen 1996	Fernandes *et al.* 2004
Enhanced vegetation Index (EVI)	$\frac{2.5(\rho_{NIR} - \rho_R)}{1 + \rho_{NIR} + (6\rho_R - 7.56\rho_B)}$ (29)	Index that minimise background reflectance and atmospheric noise and increase the sensitivity to LAI	Huete *et al.* 1994	Soudani *et al.* 2006
Reduced simple ratio (RSR)	$\frac{\rho_{NIR}}{\rho_R}\frac{\rho_{SWIR}^{\max} - \rho_{SWIR}}{\rho_{SWIR}^{\max} - \rho_{SWIR}^{\min}}$ (30)	Index that minimise background reflectance effect and increase the sensitivity to LAI	Brown *et al.* 2000	Chen *et al.* 2002; Stenberg *et al.* 2004; Stenberg *et al.* 2008

ρ is reflectance/radiance in near infrared (NIR), red (R), shortwave infrared (SWIR) and blue (B) spectral bands; L is a correction factor for soil; a and b are soil line parameters; ψ is a parameter to represent aerosol; SWIR max and min are the maximum and minimum values of SWIR reflectance/radiance for that land cover, respectively.

To this regard, Fernandes & Leblanc (2005) have demonstrated the modified least squares and Theil-Sen regression analysis to provide analytical approximations of their prediction confidence intervals in the presence of measurement errors. Besides, Berterretche *et al.* (2005) has shown that reduced major axis orthogonal regression model can be implemented to account errors both in dependent (LAI) and independent (SVI) variables. Berterretche *et al.* (2005) has also shown Geostatistical techniques (kriging with an external drift and sequential Gaussian conditional simulation) for mapping LAI although such an approach requires a distribution and density of primary, reference LAI measurements that are impractical to obtain.

Empirical modelling of LAI from remotely sensed radiometric measurement is not only restricted to SVI. Cohen *et al.* (2003) provided a tool to circumvent a limitation of LSR by constructing an integrated index to represent multiple predictor variables in a simple linear context. This index, called canonical correlation analysis (CCA) was later proven to be powerful tool for empirical retrieval of LAI (Lee *et al.* 2004; Heiskanen 2006). Hall *et al.* (1995) and Peddle *et al.* (1995) were among the first to empirically exploit the relationship between object structure and shadow characteristics for the estimation of leaf area index. Seed and King (2003) later demonstrated the relationship between shadow intensity and geometry, and spectral mixture analysis with leaf area index. To this date, empirical LAI retrieval method in one or combined form of the aforementioned statistical techniques remains to be the most common approach for LAI retrieval from remote sensing data.

Empirical models developed for application to remotely sensed optical data rely on physically based relationships between LAI and canopy spectral reflectance (Section 1.1). For example, in the near infrared region the spectral reflectance and transmittance of the leaves is high and absorptance is low. In this situation leaves from lower canopy layers contribute considerably to total measured reflectance (Clevers 1989). A common procedure to estimate LAI is to establish an empirical relationship between SVI and LAI by statistically fitting measured LAI values to the corresponding SVI. The statistical fitting is mainly carried out using LSR, whereby their generic form is expressed as:

$$LAI = f(SVI) \quad (31)$$

Theoretically, equation (31) should have been formulated in reverse order (IV). SVI is the function of LAI but not vice versa as usually reported in a vast amount of literature. The major advantage of the SVI based empirical approach over physically based reflectance or canopy models is its simplicity and ease of computation. In practice, SVI based empirical LAI prediction from remotely sensed data faces two major difficulties: (a) SVI approaches a saturation level asymptotically when LAI exceeds a certain value, depending on the type of SVI, and (b) there is no unique relationship between LAI and a SVI of a choice, but rather a family of relationships, each a function of chlorophyll content and/or other canopy characteristics, soil background effects and external conditions (Colombo *et al.* 2003; Houborg *et al.* 2007). Since there is no universal SVI-LAI equation applicable to diverse vegetation type, it is difficult to use the empirical LAI modelling with large scale remote sensing images. Considering these limitations and the theoretical formulation of SVI-LAI relationships, SVI predicting power and stability can be assessed based on (IV):

$$SVI = f(LAI) \quad (32)$$

Equation (32) can be used to localise the SVI-LAI solutions. To this regard, studies have put forward sensitivity analysis of SVI to LAI as a function of LAI, e.g., Baret & Guyot (1991) developed the relative equivalent noise (REN), Huete *et al.* (1994) employed the vegetation equivalent noise (VEN) to represent noise in SVI, Becker & Choudhury (1988) developed the relative sensitivity (R) based on the regression function of two rescaled SVIs, Gitelson (2004) proposed a wide dynamic range vegetation index, and more recently Ji & Peters (2007) demonstrated a new sensitivity function. The sensitivity function as a function of LAI are required at each observation because the goodness-of-fit measures such as the coefficient of determination (R^2) and root mean squared error (RMSE) are only useful for indicating the general sensitivity of the SVI. The sensitivity of a SVI to a LAI is not a constant value, but is a function of the LAI. However, to this date, there is no attempt at mapping LAI based on the sensitivity functions. This entails the need for LAI mapping based on the experimental and theoretical sensitivity of SVIs to various ranges of LAI (IV).

2.3 Large scale inversion of leaf area index

Over the past few years, several operational systems have been introduced for the large scale retrieval of LAI on a regional or global scale using medium resolution optical sensors with pixel sizes ranging from 250 m to 7 km (e.g., from NOAA/AVHRR (National Oceanic and Atmospheric Administration/Advanced Very High Resolution Radiometer): Los *et al.* 2000; CYCLOPES from SPOT/VEGETATION: Baret *et al.* 2007; from TERRA-AQUA/MODIS: Yang *et al.* 2006; from ENVISAT/MERIS (Environmental Satellite/MEdium Resolution Imaging Spectrometer): Bacour *et al.* 2006). Such novel approaches are based on the inversion of radiative transfer models which describe the physical interaction between incident solar radiation and vegetation canopy elements. The retrieval algorithms used in these global approaches are usually optimized for the characteristics of the sensor at issue and for the biome types found at a global level and the accuracies are always arguable (e.g., MODIS progressive overestimation: Fang & Liang 2005; Abuelgasim *et al.* 2006; Heinsch *et al.* 2006; Yang *et al.* 2006; Pisek & Chen 2007).

The mathematical and physical sophistication of the techniques used to retrieve LAI have increased considerably evolving from simple empirical (Section 2.2) to physically based approaches based on our understanding of the radiative regime of vegetation canopies. Physically based approaches for any medium can be explained in the following simple radiation budget expression:

$$\varepsilon_U + \varepsilon_T + \varepsilon_A + \varepsilon_R = 1 \quad (33)$$

were a photon striking diffusing layer either passes the layer unintercepted (ε_U), or it is scattered forward/transmitted (ε_T), or it is absorbed inside the layer (ε_A), or it is scattered backward/reflected (ε_R). For example, equation (2) describes this principle in simplest Beer's law where the extinction coefficient k is related to the energy lost by absorption (ε_A) and scattering ($\varepsilon_T + \varepsilon_R$) whilst the gap fraction equals ε_U. There have been more efforts to describe radiation transfer in vegetation using physically based modelling those link canopy properties with sensor-measured radiance. These models all work to solve the equation (33) and to retrieve critical canopy properties. In a broad category, they can be grouped as: (a) radiative transfer models, (b)

geometric optical models, (c) computer simulation models, and (d) hybrid models. One may argue, but the empirical modelling of LAI could be categorised as the simplest form of radiative transfer modelling where the parameters determined empirically/statistically not physically whilst explaining the physical relationships between variables. The radiation interactions in canopies are mainly influenced by canopy optical and structural properties, and illumination and viewing geometries. Radiative transfer and geometrical optical models define a canopy as a set of statistical ensemblages over a volume averaged properties, whereas computer simulation describe the photon trajectory and complex radiative regime of the canopy for a given radiometric attribute of a plant primitives. Therefore, the term deterministic (non-stochastic) can be applied for the former two model types. Often, the hybrid models are the combination of radiative transfer and geometrical optical models.

One of the most notable canopy reflectance models is that of Suits (1972) in which canopy is assumed to consist of only vertical and horizontal leaves and the model is characterized by canopy structure and viewing and illumination geometry. Verhoef (1984) developed the SAIL (Scattering by Arbitrary Inclined Leaves) by extending the Suits (1972) model to allow variation of leaf angles to simulate the bidirectional reflectance factor of turbid medium plant canopies, by solving the scattering and absorption of four upward/downward radiative fluxes. Among all the radiative transfer models, the SAIL canopy bidirectional reflectance model and its derivatives (see the list Jacquemoud *et al.* 2009) are the most popular once. The radiative transfer models have variable degrees of defining canopy structural configuration (e.g., LAI and leaf angle distribution (LAD)). In radiative transfer models, canopy is assumed to be a turbid medium, canopy elements are randomly distributed. In 1D case, canopy is horizontally homogeneous and infinite but vertically variable and finite (e.g., SAIL model). In case of horizontal heterogeneity and discontinuous canopies, the turbid medium analogy does not hold true. Gastellu-Etchegorry *et al.* (1996) put forward DART (Discrete Anisotropic Radiative Transfer) model to suit a heterogeneous canopy by dividing the canopy into a rectangular cell matrix based on the canopy model developed first by Kimes & Kirchner (1982). Myneni *et al.* (1990) explored and demonstrated 3D canopy radiative transfer models and their association with SVI and biophysical parameters although solving these models is complicated. To this regard, Nilson and Peterson (1991) developed an approximate solution for heterogeneous canopies by extending single scattering component. Kuusk (1995) later developed Markov canopy reflectance model based on related philosophy. There are two methods of solving radiative transfer equation, i.e., numerical and approximation (details: Liang 2004).

Most radiative transfer modelling in vegetation usually focuses in canopy level, by either using actual measurement or leaf optical models to represent scattering elements (leaves). A 'Plate' model known as PROSPECT is perhaps the most widely used leaf reflectance model particularly for broadleaf (Jacquemoud & Baret 1990). The use of PROSPECT for conifer needles inhibited due to the problems of needle shape, thickness and internal cell structure. Dawson *et al.* (1998) developed the LIBERTY (Leaf Incorporating Biochemistry Exhibiting Reflectance and Transmittance Yields) model that allows the characterization of conifer needles, at the cellular scale. Leaf reflectance and transmittance models such as ray tracing model (e.g., RAYTRAN: Govaerts and Verstraete 1998), stochastic model based on Markov chain theory (e.g., LFMOD1 model: Tucker & Garratt 1977; SLOP (Stochastic model for Leaf Optical Properties) model: Maier *et al.* 1999), and turbid medium model

based on Kubelka-Munk theory (e.g., LEAFMOD (Leaf Experimental Absorptivity Feasibility MODel) model: Ganapol *et al.* 1998) have been also demonstrated although rarely used. These effort shows that it is indispensable to model the optical property of the scattering elements in canopy radiative transfer models.

Geometric optical models use geometric optics to compute the reflectance from a plant canopy as a function of various structural (e.g., tree shape, tree height) and spatial parameters (e.g. stand density) represented by a series of regular geometric shapes (e.g., cylinders, spheres, cones, ellipsoids). Various scenes are modelled as varying proportions of shadowed and illuminated tree crowns, and shadowed and illuminated background. Most of geometric optical models in remote sensing application have been reviewed by Chen *et al.* (2000). Such models are appropriate for and have been successfully used in microwave (Sun & Ransom 1995) and LIDAR (Sun & Ransom 2000) which are out of the scope of this dissertation. Canopy geometric optical models often incorporated with radiative transfer theory forming hybrid model for LAI inversion (e.g., GORT (Geometric-Optical Radiative Transfer): Li *et al.* 1995; five-scale model: Leblanc *et al.* 1999; directional reflectance model: Kuusk & Nilson 2000; GeoSAIL: Huemmrich 2001).

Computer simulation models are another set of physically based approaches most often work based on light transport and rendering concepts. The Monte Carlo Ray Tracing (MCRT) based on sampling of photon trajectories within canopies (Arai 2000) and the radiosity (adopted for canopy by Borel *et al.* (1991) and Goel *et al.* (1991)) methods are the classical examples of computer simulation models. Very few studies have applied computer simulation model for direct biophysical parameter retrieval (e.g., radiosity: Garcia-Haro *et al.* 1999). Although requiring intensive computing resources, these models allow a more realistic representation of the vegetation canopy and a primary tool to understand radiation regime and validating other radiative transfer models.

In recent years, a theory based on the spectral invariant property of leaves and canopies expressing simple algebraic combinations of leaf and canopy spectral transmittance and reflectance becoming wavelength independent and determining a small set of canopy structure specific variables has been applied to retrieve LAI (details: Huang *et al.* 2007). The set includes the canopy interceptance, the recollision and the escape probabilities. These variables are proven to specify an accurate relationship between the spectral response of a vegetation canopy to the incident solar radiation at the leaf and canopy scales. The concept (*p*-theory) which was first introduced by Knyazikhin *et al.* (1998), describes that the amount of radiation scattered ($\varepsilon_T + \varepsilon_R$) by a canopy depends only on wavelength and spectral invariant canopy parameter called recollision probability. This parameter can be derived from gap fraction data as an average canopy value. Stenberg (2007) has shown that the recollision probability derived from gap fraction data using simple analytical formula was strongly correlated with that of simulated with Monte Carlo model. Rautiainen & Stenberg (2005) have demonstrated a new semi-physical forest reflectance model called PARAS to account the effect of within shoot scattering in coniferous canopy reflectance which has been overlooked. The PARAS model uses a relationship between photon recollision probability and LAI for simulating forest reflectance. The recollision probability is wavelength independent variable defined as the probability with which a photon scattered in the canopy interacts with a phytoelement again. This, relatively new modelling approach, has experimentally been proven to be a powerful tool for LAI retrieval (Rautiainen *et al.* 2009).

Radiative transfer modelling (including coding) in vegetation canopies has been a time consuming and labour intensive process that has been exacerbated to be challenging by lack of absolute reference standards and benchmarking. Currently, the radiative transfer scientific communities are actively participating, exchanging and evaluating their models thanks to RAdiation transfer Model Intercomparison (RAMI) exercise which developed RAMI On-line Model Checker (ROMC) tool (Widlowski *et al.* 2008). The recent RAMI is extended to evaluating bidirectional canopy reflectance models, light transmission and absorption models, as well as models capable of simulating waveform LIDAR signals and thresholded hemispherical photographs in two test environment (abstract and real canopies).

From the beginning of optical remote sensing, physically based models have helped in the understanding of light interception by plant canopies and the interpretation of vegetation reflectance in terms of biophysical characteristics. Since they attempt to describe absorption and scattering, the two main physical processes involved in such a medium, they are useful in designing vegetation indices, performing sensitivity analyses, and developing inversion procedures to accurately retrieve vegetation properties from remotely sensed data (Jacquemoud *et al.* 2009). Optimisation, inversion methods, generic algorithms and parametric and nonparametric approaches to retrieve LAI from physically based approaches are described in detail by Liang (2004). A physically based modelling approach based on a set of radiative transfer equations or models involves inverting a model:

$$r = f(LAI, ...) \quad (34)$$

where LAI is an input parameter to the model and r is the model output usually reflectances, or radiance. The inversion procedure is a process in which the model is run in a reverse mode, that is, the inputs to the inversion procedure are the reflectances (r) and the output is a set of the parameters. The inversion procedure is an ill-posed process by nature due to measurement and model uncertainties and because different combinations of model parameters may correspond to almost identical spectra (Combal *et al.* 2002). Thus, additional input information is needed to accurately estimate the vegetation parameters. The model input parameters may include soil reflectances, canopy architectures and optical properties, geometric configuration of the sensing systems, illumination conditions as well as single scattering albedos of individual leaves, leaf inclination distribution, and anisotropic properties of both canopy and soil substrates. The selection of the input parameters for the inversion of physically based models is complicated, and the parameterisation techniques typically rely on the existence of experimental data collected at the site of interest which is not usually readily available. One of the earliest attempts to retrieve vegetation parameters by inversion of canopy reflectance models can be noted from Kuusk (1998). This study has shown the difficulties of inverting radiative transfer model for large scale vegetation parameter retrievals.

A major advantage of the reflectance modelling approach is that it is a physically based approach and is independent of vegetation type. A simplified form of physically based modelling is the utilisation of Beer's law which describes the interception of radiation by plant canopies. Theoretical considerations (Clevers 1989; Baret & Guyot 1991) confirmed by some experimental observations (Wiegand *et al.* 1990, 1992; Richardson *et al.* 1992; Gutman & Ignatov 1998; Jiang *et al.* 2006) showed that most SVIs can be approximated as a simple exponential function of LAI:

$$SVI = SVI_{\infty} + (SVI_{back} - SVI_{\infty})\exp(-kLAI) \quad (35)$$

where SVI_{back} and SVI_{∞} are the SVI values for the soil (LAI = 0) and for infinite LAI (asymptotic value) , respectively. The combination of equations (2) and (35) leads to the following generic relationship between the vertical gap fraction and a SVI:

$$Po = \frac{SVI - SVI_{\infty}}{SVI_{back} - SVI_{\infty}} \quad (36)$$

Therefore, LAI can be inferred as:

$$LAI = -\ln\left[\frac{SVI - SVI_{\infty}}{SVI_{back} - SVI_{\infty}}\right] / k \quad (37)$$

Equation (37) is essentially physically based LAI modelling as the constants SVI_{∞}, $SVI_{back,}$ and k are physically determined parameters. All the required parameters can be obtained from remotely sensed images because of the high contrast that exists between soil and vegetation optical properties and because the gap fraction is a synthetic variable resulting from the combination of LAI and leaf orientation that governs directly the radiative transfer process (V–VII). This approach takes the advantages of the SVI virtues as used in empirical modelling and simplistic approach to the classical inversion of physically based radiative transfer models, where the classical dilemma between the number of independent measurements performed and the number of variables to be estimated is no longer critical. This technique can be enhanced provided that high spatial resolution remote sensing imagery is available to distinguish gaps from canopy (V; VI). Model simulations have shown that the nadir remote sensing signal may be more related to the effective LAI than to the true LAI (Chen & Cihlar 1996), indicating the importance of clumping index (VI; VII).

The LAI inverted based on equation (37) comprises optical properties of the entire vertical profile of the canopy including understorey, which is more relevant compared to ground based optical determination or purely theoretical radiative transfer formulations. However, the green LAI (due to SVI relation with optical thickness of the vegetation) from this large scale inversion algorithm might have to be converted to a geometrical parameter such as LAI determined for example from hemispherical photography. Methods for specification of SVI_{∞} and SVI_{back} are not satisfactory to the author's knowledge to this date (VII). Besides, varying orthogonal and ratio based SVIs have different sensitivity to the atmospheric effect and the spatial resolution of the remotely sensed pixels (VII). These limitations of such a simplistic and functionally relevant approach for LAI inversion require further study for the improvement (V–VII).

Large scale clumping index retrieval

Foliage element clumping is an important canopy structural parameter affecting both the gap fraction for the same LAI, radiation interception and distribution within the canopy, which in turn affects photosynthesis. Large scale clumping index retrieval has been a challenging task owing to difficulties of representing geometric property of canopy from remotely sensed optical data. MODIS LAI algorithm for example accounts for clumping at the canopy and leaf (shoot) scales through 3D radiative transfer formulations and assumptions on canopy architecture specific per biome class

(Knyazikhin *et al.* 1999). The clumping at the landscape scale can partially be addressed via mechanisms based on the radiative transfer theory of canopy spectral invariants (Knyazikhin *et al.* 1998).

Lacaze *et al.* (2002) was perhaps the first to attempt retrieving large scale clumping index from multiangular POLDER (POLarization and Directionality of the Earth's Reflectances) dataset. They have demonstrated clumping index calculations using only a portion of the BRDF, in particular, the two directional signatures, which are the maximum (ρ_{HS}: hotspot) and the minimum (ρ_{DS}: darkspot) of reflectance observed in the backscattering and forward scattering regions, respectively. A directional hot–dark spot index (HDS) is formulated using these two signatures as:

$$HDS = (\rho_{HS} - \rho_{DS}) / \rho_{DS} \quad (38)$$

It has been shown that the HDS is related with the foliage clumping index for three different vegetation types (Conifer, broadleaf and grassland). Later, HDS was found out to be empirically related with clumping index non-linearly. Therefore, Chen *et al.* (2003) suggested new anisotropy index by modifying HDS called normalised difference between hotspot and darkspot (NDHD) which was demonstrated in earlier work by Leblanc *et al.* (2001). The difference in the reflectance at hotspot and darkspot is normalized against that at the darkspot to reduce the influence of leaf optical properties on the index so that only canopy geometry will have influence in NHDS in contrast to HDS. The modified anisotropy index is:

$$NHDS = (\rho_{HS} - \rho_{DS}) / (\rho_{HS} + \rho_{DS}) \quad (39)$$

Both HDS and NHDS are being used to retrieve large scale clumping index using empirical coefficients fitted with ground based clumping index measurements. The rationale behind the relationship between clumping index and darkspot is because of clumped canopies cast dark shadows and decrease the darkspot reflectance (Leblanc et al., 2005). However, in areas of significant slope, the BRDF will no longer be symmetrical about the principal plane. Therefore, NHDS is highly biased by topographic influence due to shadowing, adjacent hill illumination, sky occlusion, and slope orientation with respect to the BRDF if complex terrain is not accounted for BRDF reconstruction. Contrary to the rich information content of multiangular imagery and the obvious future development of new instrumentation, atmospheric correction of multiangular data is troublesome. Besides, it is difficult to obtain multiangular cloud free measurements as often as single angle measurements. The commonly used radiative transfer codes for atmospheric correction are based on a plane-parallel atmosphere approximation causing problems for large view and illumination zenith angles. It is perhaps analytically challenging to decouple surface and atmospheric radiative transfer effects to retrieve surface directional reflectance property from large swath multiangular satellite instruments. To this regard, Papers VI & VII demonstrate the new look at computing clumping index from remotely retrieved gap fraction data using single view angle measurements. It is however important to acknowledge the potential of multiangular measurements to derive structural indices and a great deal of improvement on the HDS based approaches.

3. METHODOLOGY

3.1 Study areas

The study areas of this dissertation concentrate on two regions, one located in Taita Hills, South-East Kenya (I–III; Figure 3) and another in Gatineau Park, Southern Quebec, Canada (IV–VII; Figure 3). The study areas are chosen based on the on-going monitoring research activities (Pellikka *et al.* 2000b, 2009; Olthof *et al.* 2001, 2003, 2004; King *et al.* 2005; Pasher & King 2006; Pisaric *et al.* 2008), complex topography, and dense vegetation which create ideal test sites for enhancement and robustness assessment of LAI retrieval from remotely sensed data.

The forest fragments of Taita Hills, South-East Kenya (03°15′–3°30′S and 38°15′–38°30′E) are located on the dry Serengeti plains approximately 165 km inland from the Indian Ocean. The studied forest fragments include Ngangao, Chawia, Fururu, Yale, Mwachora, and Macha (Figure 3(c)). The forest fragments are characterized by tropical cloud forest with typical indigenous tree species such as *Tabernaemontana stapfiana*, *Albizia gummifera*, *Phoenix reclinata*, *Xymalos monospora, Macaranga conglomerata, Syzygium guineense*, *Cola greenwayi, Maesa lanceolata, Lepidotrichilia volkensii* (Chege & Bytebier 2005; Rogers *et al.* 2008). In addition, *Cupressus lusitanica*, *Eucalyptus saligna, Pinus elliottii*, *Pinus caribea*, *Pinus patula,* and *Grevillea robusta* are common exotic species found in most of the fragments (Pellikka *et al.* 2009). The altitudinal range of the forested area is from 1500 to 2200 m. In order to determine a broad range of forest types, data were collected from natural tropical cloud forests with dense overstorey, dense understorey and sparse overstorey; and *Pinus*, *Cupressus,* and *Eucalyptus* spp. plantations. The sampling design was setup to include contrasting forest types, varying canopy structure and topography. Photosites were located randomly away from the forest edge stratified by forest types of each fragment. The minimum distance measured between two adjacent photosites was 9.5 *m*. All the fragments have varying aspects and slopes. The number of photosites was proportional to the size of the fragments.

Gatineau Park (Figure 3) is managed by the National Capital Commission (NCC) of Canada and centred at 45°30’N, 75°52’W. The park is about 10 *km* by 50 *km* and is mostly temperate hardwood forest with a dominant overstorey of sugar maple (*Acer saccharum* Marsh.) and small patches dominated by American beech (*Fagus grandifolia* Ehrh.), trembling aspen (*Populus tremuloides* Michx.), and red oak (*Quercus rubra* L.). Small numbers of red maple (*Acer rubrum* L.), American basswood (*Tilia americana* L.*),* ironwood (*Ostrya virginiana* (Mill.) K. Koch), white ash (*Fraxinus americana* L.), black ash (*Fraxinus nigra* Marsh.), white birch (*Betula papyrifera* Marsh.), and black cherry (*Prunus serotina* Ehrh.) are also present. The study plots were located in the southern portion of the park (Figure 3 (c)). In 1998, 61 plots, each 20 m by 20 m, were placed on two north-south oriented transects in the Gatineau Park for the ice storm damage studies (Pellikka *et al.* 2000b). Fifty-four of these plots that could be easily found in 2007 were selected. Plot corners were surveyed using differential global position system (GPS) to provide positional accuracy on the order of <1 m. The forests of the Gatineau Park were damaged badly by an ice storm occurring in 1998, but the park authority NCC did not clear the damaged trees and wood from the forest. The forest damage, structure, health and succession are the topics of on-going monitoring research activities in Gatineau Park (Pellikka *et al.* 2000a; King *et al.* 2005).

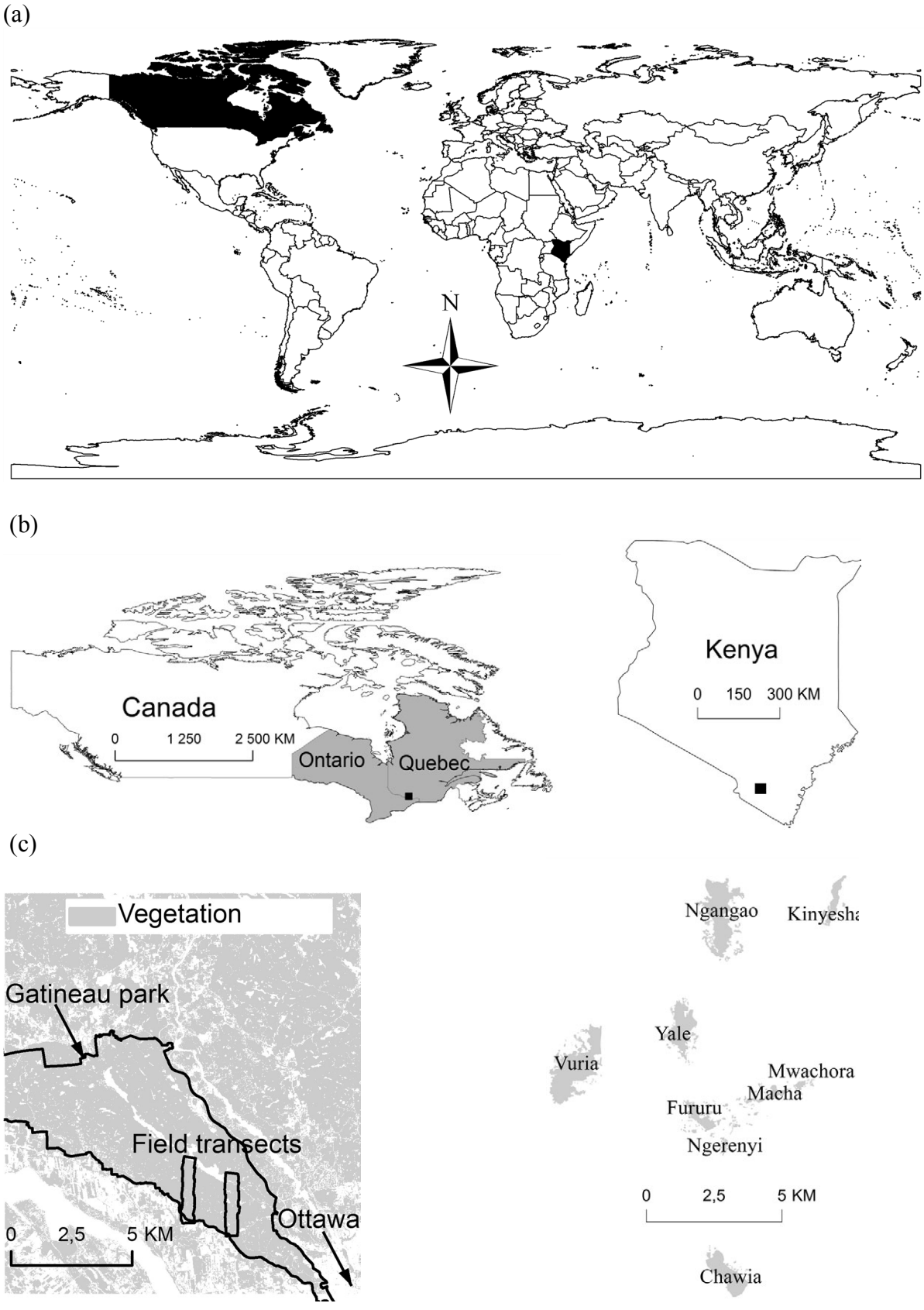

Figure 3. *(a) Relative locations of Canada and Kenya in dark gray, (b) relative locations of study sites within Canada and Kenya, and (c) locations and extents of the study areas of Papers I–VII.*

3.2 Data

Table 6 summarises the datasets used in the dissertation and the corresponding Paper. The following sections describe the details of datasets and preprocessing procedures.

Table 6. *Field, simulated and remote sensing datasets used in the original Papers.*

Data	Paper
Close-range remote sensing data: hemispherical photography, Taita Hills	I–III
Close-range remote sensing data: hemispherical photography, Gatineau Park	IV–VII
Simulated hemispherical photography data	I; III
Airborne remote sensing: colour digital imagery	VI; VI
Airborne remote sensing: colour infrared (CIR) digital imagery	V; VI
Satellite remote sensing data: SPOT 5 HRG imagery	IV; VII
Satellite remote sensing data: MODIS LAI product	VII
Simulated spectral data: PROSPECT and SAIL	IV; VII

3.2.1 Close-range remote sensing data

A total amount of 184 (92 pairs) hemispherical photographs were taken in a series of forest fragments in Taita Hills between 4th and 10th February 2007 (I–III; Figure 3(c)). The photographs were acquired using a high resolution (8 mega pixels) Nikon coolpix 8800 VR digital camera equipped with a fish-eye Nikon FC-E9 lens adapter under overcast conditions to minimize the anisotropy of the sky radiance and to reduce the scattering fluxes in the digital image. The camera was mounted on a tripod to facilitate different camera settings: to orient the photograph acquisition and to take the aspect of slope direction. Two types of photograph were taken from each sampling point in the forest fragments of Taita Hills: (a) 'levelled' to horizontal using a spirit-level and (b) 'tilted' normal to slope (the lens oriented parallel to the slope direction). For each sampling point, the slope magnitude and direction were measured. In order to take tilted photographs, the fish-eye lens was tilted towards the downslope direction using a spirit-level, compass, measuring string, lens cover and protractor. The camera was set at height of 1.3 *m* above ground. Both types of photographs (levelled and tilted) were acquired within the shortest possible time with the same manual aperture and shutter speed for the same sampling point to avoid the altering light regime. These photographs were used for sampling of gap fraction for LAI and clumping index calculations (I), for slope corrections (II), and clumping index computations (III). Different vegetation types and slope classes were represented by sufficient sampling measurements.

In Gatineau Park, the ground LAI measurements were collected using digital hemispherical photography between August 10th and 20th, 2007 using the same digital camera and lens mentioned above. In total, five photographs were acquired in each study plot, one at each corner and one at the centre. The camera was mounted and levelled on a tripod at a height of 1.3 *m* above ground. These photographs were used in the Papers IV–VII as a validation dataset.

3.2.2 Simulated hemispherical photography data

A set of hemispherical photographs were simulated to investigate the effect of resolution of sampling grid on LAI computation based on different fractional clumping and LAI (I), and the computation of foliage clumping index following various gap fraction and size theories (III). The photographs were simulated within a *3D* forest stand for a range of simulated, true LAI values 2, 4 and 6, and clustering percentage (fractional clumping, *Fc*) ranging from 0 to 1 by increments of 0.1 providing a total of 33 combinations. For details and procedures on simulating *3D* spatial distribution of foliage, i.e., foliage clumping refer to the work of Walter *et al.* (2003). Simulation of foliage clumping was done in three steps (Fournier *et al.* 1996): (a) calculating foliage distribution within a *3D* matrix by specifying the total LAI, *Fc*, and the number of cluster seeds or centres, (b) simulating a horizontally extended canopy, and (c) applying a ray tracing algorithm. Calculations were applied to a rectangular volume with 5 m per horizontal side and 10 m of height and composed of small opaque cells with dimensions of 10 cm per horizontal side and 1 cm of height. Cells simulated a horizontal flat leaf with a thickness of 1 cm. The number of opaque cells was calculated from the total LAI selected while taking into account an LAI contribution of each 0.01 m^2 cell. *Fc* is a percentage applied to the Euclidean distance separating a leaf from its closest clump centre. $Fc = 0$ corresponds to a random foliage element distribution. The forest stand was simulated by placing side to side, with no space, a copy of the same *3D* volume until sufficient horizontal extent was reached. The bases of the volumes were placed at a height of 10 *m* to simulate a vertical distribution of foliage between 10 and 20 *m*. A 600 $m \times 600$ *m* forest stand was simulated to reduce the border effects at large view angles. These photographs were used in Paper I and III. The photographs were simulated at the centre of the stand at 1.5 m above the ground to recreate a possible scenario. The ray tracing simulations resulted in an image formed only by black (0, obstructed ray) and white (1) pixels.

3.2.3 Airborne remote sensing data and preprocessing

A data set of colour and colour infrared (CIR) digital camera images was captured on a cloud free day of the 21st of August 2007, between 12:32 and 13:24 local time, from an aircraft flying at approximately 309 *m* above ground level in Gatineau Park (Figure 3(c)). During the acquisition, the solar zenith angle was between 34.3^{o} and 33.6^{o} and the azimuth angle was between 164^{o} and 188.1^{o}. The CIR camera was a Duncantech MS4100 with 1920 x 1080 pixel format and a 24 mm lens. It is a 3-CCD (charge-coupled device) camera with dispersion optics that split incident irradiance into three bands: green (500–600 *nm*), red (600–700 *nm*) and NIR (750–850 *nm*). The colour camera was a Nikon D200, a single CCD with 3872 x 2592 pixel format and a 28 mm focal length lens. Exposures were set before each flight line to optimize the dynamic range and to result in image motion during each exposure of less than ½ a pixel. Exposure intervals for both cameras were set to provide 60% forward overlap. The nominal ground pixel size was 60 cm for the CIR data and 35 cm for the colour data. The images were georectified using 25 cm pixel orthophotos provided by the NCC. An average of 10 ground control points (GCPs) was selected for each image. A 1st-order polynomial and nearest neighbour interpolation were used as the warping and grey level resampling methods, respectively. The output projection for the registered images was Universal Transverse Mercator (UTM) zone 18 with a North American Datum 1983 (NAD83) datum. Mosaics were assembled using pixels in the overlap

area of each image pair that were closest to nadir. This minimized the effect of the bidirectional reflectance distribution function (BRDF), vignetting and light-fall off (Pellikka 1998; Lévesque & King 1999; Pellikka *et al.* 2000b). The mosaics were also clipped from each side to restrict the across track view angle to 8^{o}. The ground plots were distributed along the centre of the mosaic (flight line) so the between plot optical variation was minimized. Both colour and CIR airborne imagery were used in Papers V &VI for large scale LAI inversion algorithms.

3.2.4 Satellite remote sensing data and preprocessing

Two sets of satellite datasets were used in Papers VI & VII. The first one was SPOT 5 HRG (Satellite Pour l'Observation de la Terre 5 High Resolution Geometric) imagery in radiances in digital counts in the green (500–590 *nm*), red (610–680 *nm*), NIR (780–890 *nm*) and SWIR (1580–1750 *nm*) wavelength regions in 10 *m* resolution acquired on cloud free day of July 23, 2007, 10:49 local time for 60 *km* × 60 *km* image swath. The sun zenith and azimuth angles were 30 and 140 in degrees, respectively. The view zenith angle was 20 degree. The SWIR band is originally acquired at 20 *m* pixel size and resampled into 10 *m* in order to match other bands. The SPOT image was obtained from the OASIS program financed by the European Commission, DG Research. The image was orthorectified using a 3 arc seconds digital elevation model (DEM) obtained from Canadian Digital Elevation Data (CDED) based on SPOT XS sensor colinearity geometric model. The SPOT image was registered using 139 GCPs from orthorectified digital aerial photography and national road network of Canada into UTM zone 18 with a NAD83 datum. The radiance was calibrated and corrected using five atmospheric correction techniques: namely, four dark object subtraction (DOS) techniques (Song *et al.* 2001) and radiative transfer code developed by Vermote *et al.* (1997) called second simulation of the satellite signal in the solar spectrum (*6S*).

The second satellite dataset was MODIS Collection 5 LAI product acquired in a form of Hierarchical Data Format (HDF) subsets from the Warehouse Inventory Search Tool (WIST) client. The subset LAI product was in 1 *km* resolution with 8 days composite using maximum fraction of photosynthetically active radiation (FPAR). The HDF subset was re-projected and they matched the study area layout. The available LAI was downloaded from date 23/07/2007 (20 – 27/07/2007) to cover the same period of ground and SPOT data acquisitions in Gatineau Park. Only pixels retrieved with the main algorithm without cloud contamination were used in Paper VII (Myneni *et al.* 2002).

3.2.5 Simulated spectral data

The combined PROSPECT leaf optical properties model (Jacquemoud & Baret 1990) and SAIL turbid medium canopy bidirectional reflectance model (Verhoef 1984), also referred to as PROSAIL, were used in order to evaluate the spectral sensitivity of SVIs to LAI (VI) and to test the robustness of the methodologies developed in Paper VII. The canopy reflectance was simulated for three wavelength bands centred around 645, 834 and 1645 *nm*, corresponding to red, NIR and SWIR bands of SPOT 5 HRG, for a range of plausible input parameters. PROSPECT uses the following input parameters: chlorophyll *a* and *b* content (*34.2* $\mu g.cm^{-2}$), dry biomass content (0.0045 $g.cm^{-2}$), equivalent leaf water content (*0.0137* $g.cm^{-2}$), and mesophyll structure parameter (1.55 *N*); and SAIL uses: LAI, leaf angle distribution (spherical), soil

reflectance and external parameters like Sun zenith (0^o), view zenith (30^o) angles, and Sun and view azimuth angles (0^o). For this analysis, the ranges of the LAI inputs were; 0.25 – 9 by increment of 0.25, and 12 to represent the largest LAI value. Three different soil backgrounds ranging from dark to bright were specified from Bowker *et al.* (1985). The other input parameters were kept constant as specified above in parenthesis. The input parameters which have been used in the analysis are within the realistic range and adopted from other simulation studies (Jacquemoud & Baret 1990; Jacquemoud *et al.* 2000).

3.3 Leaf area index determination from ground measurements

Remote sensing of LAI is challenging field of study due to the temporal and structural dynamics and varying structural and biochemical measurement dimensions associated with LAI. Besides, ground based optical LAI is often mistakenly perceived as a "ground truth" dataset. Ground based LAI measurements are just another metrics of LAI and their value varies significantly depending on the instrument and algorithms used (see Figure 7 in Garrigues *et al.* 2008; Gonsamo Gosa *et al.* 2007). Methodology inter-comparisons particularly for clumping index computation, correction for complex topography and sampling of gap fraction and size datasets are often overlooked in the literature. Paper I–III deals with the aforementioned research questions using hemispherical photographs from Taita Hills.

One of the crucial steps in the measurement of canopy gap fraction and/or size using hemispherical photography is determining the resolution of the sampling grid, meaning the projected image plane is divided into elements of a sampling grid, according to the geometric distortion of the fisheye lens. In Paper I, the effects of varying resolutions of sampling grids by modifying the angle widths of zenithal annuli and azimuthal sectors were evaluated and discussed for LAI and clumping index computations. Exhaustive sensitivity analysis was performed to test these effects; using artificial photographs simulating ideal canopies (Section 3.2.2). The LAI was computed using Lang's graphical and iterative method (Lang 1986). The clumping index was based on the Lang and Xiang logarithm gap averaging method (Lang & Xiang 1986). All the simulated and real photographs were analysed using CIMES-FISHEYE software (Walter 2008) in order to extract oriented gap fractions, and derive LAI and clumping index. For both simulated and real photographs, the image analysis was restricted to the zenith view angle below 60^o to avoid mixed pixels near to the horizon, which result mainly from the light scattering and coarse image resolution.

The slope effect and correction methods for estimation of canopy gap fraction, LAI, mean leaf angle and clumping index using hemispherical photography, were investigated in Paper II. The evaluation was carried out in tropical cloud forest and plantations in Taita Hills in order to consider a range of canopy architecture and slopes up to 65% (Figure 3 (c)). The two acquisition techniques and various slope correction procedures were compared. All estimates assume uniform slope, canopy parallel to ground and homogeneous canopy structure at the photosite level. The slope correction method implies the use of variable path lengths and adjusting LAI to horizontal datum. For photographs oriented to local zenith (levelled acquisition), calculations were made using: (a) fixed path lengths over azimuths using zenith reference axis, calculation and removal of sky parts of the hemisphere obstructed by topography, azimuthal inversion of gap fraction without prior averaging and deriving local LAI estimates (quasi-random model), and LAI referred to horizontal and

corrected for topographic shading, and (b) variable path lengths over azimuths using normal to slope reference axis, LAI adjusted to horizontal by dividing by the slope cosine. For photographs oriented parallel to slope (tilted acquisition), calculations were made using: fixed path lengths over azimuths, normal to slope reference axis, LAI adjusted to horizontal by dividing by the slope cosine, and azimuthal inversion of gap fraction without prior averaging deriving local LAI estimates (quasi-random model). CIMES-FISHEYE software was used for the calculations.

In Paper III, varying methodologies of clumping index determination on real hemispherical photographs, and on the simulated photographs representing different aggregation levels of foliage elements were evaluated. The comparative analysis was carried out for the effects of forest types, forest density, slope and gap fraction acquisition accuracy on estimation of clumping index using the five gap fraction averaging methods and gap size distribution theories (Walter *et al.* 2003; Jonckheere *et al.* 2004; Leblanc *et al.* 2005). CIMES-FISHEYE software was used for the calculations.

Hemispherical photograph as a ground comparison datasets for Papers IV–VII from Gatineau Park were analysed using CAN_EYE software (e.g. Demarez *et al.* 2008). LAI was computed for the range of 0^{o}–60^{o} view zenith angle using Campbell's ellipsoidal distribution function of leaf angles (Campbell 1986; Campbell & Norman 1989). Fractional vegetation cover (f_c) was extracted from the average gap fraction computed within 0^{o}–20^{o} view zenith angle. For simplicity, the effective LAI, which assumes random foliage distribution, was used in Papers IV, V & VII, and logarithm gap averaging method clumping index (Lang & Xiang 1986) in addition to LAI in Paper VI.

3.4 Leaf area index determination using empirical modelling

A spectral vegetation index is a quantitative measure usually formed from combinations of several spectral bands, whose values are added, divided, or multiplied in order to yield a single value that indicates the amount or vigour of vegetation. By and large, empirical modelling of LAI based on the SVI-LAI statistical relationships remains common method of retrieving spatially explicit LAI. In Paper IV, the performances of seven ratio based SVIs were investigated for their sensitivity to a varying range of LAI. The SVIs were selected based on the extensive use, performance and sensitivity to LAI on high vegetation cover. The SVIs include: SR (simple ratio, Jordan 1969), ISR (infrared simple ratio, Fernandes *et al.* 2003), NDVI (normalized difference vegetation Index, Rouse *et al.* 1973), NDII (normalized difference infrared index, Hardisky *et al.* 1983), RSR (reduced simple ratio, Brown *et al.* 2000), RNDVI (reduced normalized difference vegetation Index, Nemani *et al.* 1993), and RISR (reduced infrared simple ratio, IV). Most of the three band SVIs are included and ISR was extended by correcting by scaled difference of red reflectance and named reduced infrared simple ratio (RISR). The new vegetation index, RISR, significantly reduced the effect of soil background reflectance while maintaining high sensitivity to wide range of LAI. The sensitivity assessments were carried out for both SPOT data from Gatineau Park and simulated spectra. The main sensitivity function was the first derivative of the regression function divided by the standard errors of the SVI (Ji & Peters 2007). In addition, band and individual SVI sensitivity with LAI was carried out using the ordinary least squares regressions. The aim was to evaluate the applicability of multiple SVIs for LAI mapping based on the sensitivity analysis (IV).

3.5 Large scale leaf area index inversion algorithms

Theoretically most SVIs can be approximated as a simple exponential function of LAI which is confirmed by some experimental observations (Section 2.3). In Paper V & VI, large scale LAI inversion algorithms (Equation 37) were applied on the gap fraction data obtained from the colour and CIR airborne imagery from Gatineau Park (Equation 35 & 36). In Paper V, NDVI, maximum likelihood and object-oriented classifications, and principal component analysis (PCA) methods were applied to calculate the mono-directional gap fraction. The LAI inverted using the two classification methods, PCA, and NDVI were inter-compared and independently evaluated using the ground based LAI measurements. Four measures were used to evaluate algorithm effectiveness: namely, Pearson correlation coefficient, RMSE, overall average accuracy (OAA), and visual examination based the LAI maps in comparison with the CIR image to assess the overall spatial distribution of predicted LAI. The method which performed best was used for producing LAI maps for the entire mosaic covers in both sampling transects. Paper VI further explores the robustness of large scale LAI inversion algorithms from colour and CIR imagery by extending the airborne gap fraction extraction methods and developing new airborne clumping index estimation technique. Colour based thresholding procedures were used besides NDVI for gap fraction extraction. The NDVI based gap fraction was further used for computation of clumping index following logarithmic averaging method which was initially developed for ground measurements (Lang & Xiang 1986).

Paper VII further explores the applicability of large scale LAI inversion used in Paper V & VI, using red and near infrared reflectances obtained from high resolution satellite imagery (SPOT 5 HRG) over Gatineau Park. NDVI, scaled difference vegetation index (SDVI, Jiang *et al.* 2006) and modified soil-adjusted vegetation index (MSAVI, Qi *et al.* 1994) were applied to calculate mono-directional gap fractions. The robustness of the algorithms was evaluated using the ground based LAI measurements and by applying the methods for the independently simulated reflectance data using PROSAIL radiative transfer models. Furthermore, the high resolution LAI was compared with MODIS LAI product. The effects of atmospheric corrections and scales were assessed for each of the method. Thorough analysis was dedicated to accurate determination of SVI_{back} and SVI_{∞} which are the SVI values for the soil (LAI = 0) and for infinite LAI (asymptotic value), respectively (Equation 35–37).

4. GENERAL RESULTS AND DISCUSSION

4.1 Leaf area index determination from close-range optical observation: hemispherical photography

An astonishing aspect of hemispherical photography is that such a wide range of estimates of leaf area and clumping indices are produced by different methods. In earlier days, interpretation of hemispherical photography required tedious manual analysis of gap fraction sampling through overlay of clear sampling grids upon prints or the projection of photographs on an opaque sampling grid (Anderson 1964). The projected image plane is divided into elements of a sampling grid, according to the geometric distortion of the fisheye lens. Herbert (1987) provides a discussion of hemispherical projections and lens distortion corrections. Manual analysis is tedious and time consuming. Nowadays, digital image analysis techniques are being used allowing efficient analysis of large numbers of photographs. The geometric distribution of openings (gap fraction) can be measured precisely and can be used to estimate potential solar radiation penetration through openings and to determine aspects of canopy architecture such as fractional vegetation cover, LAI, clumping index, and leaf angle distribution. In hemispherical photography, gap fraction represents the relative proportion of open sky contained in any sampling grid or concentric sky ring on the projected image plane. The resolution of the sampling grid, or seldom referred to as 'sky map' is determined by the number of zenithal annuli and azimuthal sectors. Therefore, the sky map consists of their respective intersections, defining sky segments. The resolution of sampling grid affects: the probability of encountering segments which are completely blocked by canopy elements (I–III), the azimuthal averaging of gap fraction (I–III), the slope correction (II), the clumping index computations (I–III) and therefore LAI estimation (I–III).

The results (I) indicate that the LAI and clumping index estimates vary considerably for different resolutions of sampling grids from both simulated and real photographs for clumped foliage distributions. In this work, the effects of varying resolutions of sampling grids by modifying the angle widths of zenithal annuli and azimuthal sectors were evaluated for LAI and clumping index computations. A new approach to solve the problem of 'empty segments', obscured completely by foliage, is proposed. For comparative analysis, a segment with null-gap is given a value of maximum effective LAI of 8 (*LAIsat*), to compute new gap fraction following local Poisson model, a common procedure (Weiss *et al.* 2004; Leblanc *et al.* 2005). The number of sky segments does not affect the LAI and clumping index estimates as long as the foliage elements are randomly distributed. The arbitrary value of *"LAIsat"* 8 assigned for empty segments has caused the overestimation of estimated LAI compared to merging them for the simulated LAI of 2 in all numbers of sky segments where empty segment were encountered. For simulated LAI value of 6, *"LAIsat"*-based method underestimated compared to merging them for the two maximum sky resolutions of 5184 (2.5^o segment width) and 3600 (3^o segment width) due the fact that at these resolutions the proportion of empty segments is more than 50%. Merging empty segments to the following non-empty segments was proven to be a robust approach for both LAI and clumping index estimates. A segment with very small gap fraction is likely to occur near to an empty segment, which affects both LAI and clumping index retrievals, as the logarithm of a near zero gap fraction value gives an infinitely high LAI, an often overlooked problem. Therefore, merging the empty

segments with the closest non-empty segments avoids unfavourable outputs from both the zero, or near to zero gap fractions.

From simulated photographs, the higher the foliage clumping, the lower the estimated effective LAI nearly in systematic manner in all considered equiangular sky resolutions. This confirms that, increasing the number of sky segments does not per se improve the estimated LAI in order to avoid the necessity for correction parameters such as clumping indices. For random simulation of LAI 6, 18% and 21% variations between minimum and maximum effective and true LAI estimates, respectively, were obtained from *"LAIsat"*-based recalculated gap fractions for empty segments along the various numbers of sky segments. Whereas, only 4.5% and 6% variations between minimum and maximum effective and true LAI estimates, respectively, were obtained for merged empty segments. This suggest that merging empty segments rather than assigning an arbitrary *"LAIsat"* value may reduce bias and sensitivity of estimates for various numbers of sky segments for LAI estimations.

Leblanc *et al.* (2005) and Demarez *et al.* (2008) suggested the use of *"LAIsat"* value varying from 2 – 12 to recalculate a new gap fraction for empty segment using the Poisson model as used in this study. However, there is no obvious a priori reason for choosing this method and the upper saturated value of LAI. van Gardingen et al. (1999) suggested altering empty segments artificially by adding a gap of one pixel. However, there is no reason why this should work, because the one pixel gap is dependent on the pixel resolution of the photograph. If the proportion of empty segments is high, altering empty segments by adding a pixel of gap tends to decrease LAI and Ω estimates. The combined effect of this may result higher true LAI for low density and lower true LAI for higher density forest canopies depending on the proportion of empty segments and the effect on Ω. Therefore, HP analysis tools for canopy structure computation should employ a technique of merging each 'empty' segment with the following non-empty segment to produce a bigger segment with average value.

Form real photographs, there was systematic difference of estimated LAI and clumping index using different numbers of sky segments. LAI and clumping index estimates demonstrated strong and significant correlations, using various numbers of sky segments. The increase in effective LAI with increasing number of sky segments can be attributed to local heterogeneity of gap distribution, thus non-random distribution of foliage elements is partially taken into account when Lang's approach for LAI calculation is applied without gap fraction azimuthal averaging. Generally speaking, the determination of the number of sky segments that suits all canopy types was found out to be a difficult practical problem. However, Paper I presents more objective procedures for determining the sky map resolution and the workable hemisphere regions for gap fraction measurements along with theoretical considerations.

In Paper II, the slope effect and correction methods for estimation of canopy gap fraction, LAI, leaf inclination angle and clumping index using real hemispherical photography from Taita Hills, were investigated. The results are presented from two acquisition techniques: (a) photographs oriented to local zenith (levelled acquisition), and (b) photographs oriented parallel to slope (tilted acquisition). Gap fractions presented a stronger upslope/downslope asymmetry when retrieved from levelled acquisition. As a result, gap dispersion index (the relative variance of gap fractions: variance/mean × 100) and foliage clumping proved to be significantly higher for levelled acquisition ($P < 0.001$). LAI estimates adjusted to horizontal are not significantly different, whether retrieved from levelled or tilted acquisitions, up to

30% slopes. From levelled acquisition, fixed and variable path length do not yield significantly different LAI estimates along the whole slope gradient. From tilted acquisition, LAI values were systematically higher than from levelled acquisitions, the stronger the slope, the higher the difference. Average leaf inclination angles do not differ significantly ($P > 0.05$) for fixed vs. variable path lengths along the slope gradient up to 30%. For more severe slopes, variable path lengths yield lower average leaf inclination angle values. The interpretation of results from tilted acquisition remains uncertain. As a preliminary study, no preference is suggested for the levelled or tilted acquisition technique. Generally speaking, regarding the amount and distribution of gap fractions, a negative bias of gap fraction was found for upslope sectors and a positive bias for downslope sectors from levelled acquisition and was in agreement with Walter & Torquebiau (2000).

Paper III presents the results of comparative analysis of clumping index using five different methods. The methodological setup for the comparative analysis in Paper III was refined by the findings of Paper I & II. The result indicated that clumping index estimates based on gap size distribution approaches performed best and were less affected by topography and forest density compared to approaches based on solely logarithmic gap averaging method. Clumping index based on the gap size distribution theories are less affected by slope due to the fact that they are sensitive mainly for smaller gap sizes. As demonstrated in both simulated and real photographs analysis in this study, the combination of logarithmic gap averaging and gap size distribution approach is preferred in all scenarios such as varying forest density, slope and foliage aggregation. Overall, acceptable but lower correlations were obtained among varying computation methodologies and photograph acquisition techniques (*Pearson correlation coefficient < 0.5*). There was no clear difference of clumping index estimates along the severity of slope. This is due to the fact that photo point based comparison used in Paper III is biased due to the view direction changes when the lens is tilted to the parallel of sloping ground. Paper III disproved the general suggestion (Macfarlane *et al.* 2007) of the use of the logarithmic gap averaging method for correcting foliage clumping in preference to gap size theory method, unless the gap size distribution is known to be very accurate.

4.2 Leaf area index determination from remotely sensed optical observation: high resolution airborne and satellite remote sensing

Prior to large scale LAI inversion algorithm developments, traditional empirical modelling was tested for both airborne and satellite imagery. Figure 4 presents the result example of this approach for the CIR imagery over the Gatineau Park. It is evident that the correlation is too weak between NDVI and ground based LAI for mapping application of spatially explicit LAI. Therefore, no further attempt was considered for CIR imagery using empirical modelling. The main reason for the poor correlation was the denseness of the forest plots (average ground based effective LAI was 4). SVIs are known to saturate at fairly low LAI values of about 2–3 (Chen *et al.* 2002).

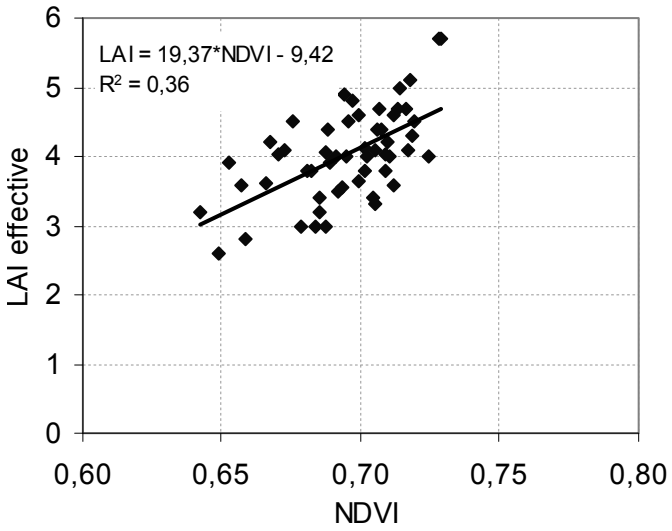

Figure 4. *Normalised Difference Vegetation Index (NDVI) vs. leaf area index (LAI). LAI effective was obtained from hemispherical photography and NDVI is calculated from colour infrared airborne imagery over the two transects of Gatineau Park (Figure 3(c)).*

Paper IV instead presents the thorough analysis of the potential of empirical modelling with spectral sensitivity analysis aimed at mapping LAI over large area. In Paper IV, two datasets were used in order to evaluate the use of the sensitivity functions for SVI-LAI sensitivity analysis and subsequently applying for LAI mapping. Analysis with PROSAIL simulation datasets illustrated the varying sensitivity of seven ratio based SVIs used in this study at various LAI ranges. There are compelling reasons to use several SVIs for LAI mapping for various ranges of photosynthetic biomass density and fractional vegetation cover. For example, Carlson & Ripley (1997) and Verstraete & Pinty (1991) described that the variation of NDVI with respect to the LAI in partially vegetated areas would be mostly controlled by the variation in the fraction of vegetated surface area illuminated by the sun and visible to the radiometer than by changes in the optical thickness of canopies. Whereas, an increasing NIR canopy reflectance at larger LAI and canopy cover is attributed to more sunlit and shaded canopy contributing to the canopy reflectance. Likewise, as the LAI and canopy closure increase, the red reflectance decreases as less of the reflective sunlit background is observed.

Analysis with PROSAIL simulation datasets illustrated the varying sensitivity of seven SVIs used in this study at various LAI ranges. The simulated datasets further indicated that several SVIs can be used for LAI mapping provided that the *S* function (sensitivity function, Ji & Peters 2007) results are large enough. It was also further demonstrated that, although *S* is statistically significant to show SVI sensitivity to LAI, it does not necessarily indicate that the relationship obtained from the *S* function can be used for LAI mapping. This was the case with the real dataset in this study where the relationships which resulted in statistically significant *S* resulted in statistically insignificant relationships when applied for LAI mapping. One of the most intriguing results in Paper IV was the ability of the newly developed index called RISR to reduce varying soil background reflectance effect for potential LAI retrieval. Moreover, Paper IV has also shown the relationships of each spectral bands, soil effect, and sensitivity assessment using classical regression functions.

Based on the results shown in Figure 4 and Paper IV, further studies were considered to retrieve LAI from high resolution airborne (V; VI) and satellite imagery

(VII). To this regard, large scale LAI inversion algorithms were developed for determining LAI of a forest located in Gatineau Park. In Paper V and VI, NDVI, maximum likelihood and object-oriented classifications, and PCA, and colour based thresholding methods were applied to calculate the mono-directional gap fraction.

Paper V and VI present the results of LAI retrievals from colour and CIR airborne imagery. There was high inter-correlation (*Pearson correlation coefficient >0.5, P<0.01*) among LAI values inverted using the classifications and PCA gap fraction extraction methods, but neither were highly correlated with LAI inverted from the NDVI method (V). LAI inverted from the NDVI based gap fraction was significantly correlated with ground based LAI (*Pearson correlation coefficient =0.63, RMSE=0.52*), while LAI inverted from the classification, thresholding and PCA derived gap fraction showed poor correlation with ground based LAI (V; VI). The LAI inverted from CIR imagery outperformed that of colour imagery in all cases.

A clumping index calculation algorithm is demonstrated using the logarithmic gap averaging method based on the gap fraction data obtained from scaled NDVI (VI). The inverted LAI true (corrected with the clumping index) was best correlated with measured LAI effective (*Pearson correlation coefficient* = 0.67, VI). This indicates that the clumping index estimated from NDVI is a meaningful physical parameter for correction of LAI even though this kind of clumping index estimation does not exist in literature. The assumption of logarithmic gap averaging method for clumping index computation is valid as long as gap sizes are concerned, which is obtained from NDVI (Lang & Xiang 1986). The gap size from gap fraction derived from NDVI can be interpreted as the possible dynamic range of the NDVI with regard to the individual pixel size. These results show that further testing of this procedure as an alternative approach for LAI retrieval from remote sensing datasets is justified.

The large scale algorithms shown in Paper V and VI were further extended to 10 *m* resolution SPOT 5 HRG imagery. Paper VII presents the results obtained from gap fraction based on scaled difference NDVI, SDVI and MSAVI indices for high resolution satellite imagery. NDVI was found to be an unsuitable index for large scale LAI inversion due to the sensitivity to scale and atmospheric effects. SDVI was virtually scale and atmospheric correction invariant. MSAVI was also found to be scale invariant. Considering all sensitivity analysis, MSAVI performed best followed by SDVI for robust LAI inversion from high resolution imagery. The clumping index algorithm shown in Paper VI once again was found to be a useful parameter particularly in correction of the scale (spatial resolution) effect on LAI (VII). MODIS LAI was overestimated compared to large scale LAI inversion from SPOT by 43% for NDVI, 232% for SDVI, and 134% for MSAVI methods. The overestimation was very severe for higher LAI values. During the late summer, MODIS LAI products show great and progressive overestimation (Pisek & Chen 2007). MODIS LAI products are known to overestimate LAI, for example, upto 75% (Yang *et al.* 2006), 200% over Canada (Abuelgasim *et al.* 2006), by 2 – 3 LAI over BOREAS study area in Canada for broadleaved forest (Fang & Liang 2005) and upto 323.6% across north American forest sites (Heinsch *et al.* 2006).

Generally speaking, the overall effectiveness assessment shows that LAI can be estimated in a robust way using the information contained on the image scene alone. However, the varying definitions and assumptions used for LAI obtained from ground based measurements, airborne images, SPOT image and MODIS product, and the validity of using simple *1D* radiative transfer model (PROSAIL) for robustness assessment make impossible any complete validation of the approaches (V–VII). The ground based measurements give the "plant area index" which includes non-

photosynthetic parts of plants such as braches and stems. On the other hand, the LAI retrieved from SPOT and airborne CIR imagery refer to the "green leaf area index" which is highly relevant from application and vegetation function point of view for photosynthesis, evapotranspiration and carbon balance studies. The green LAI can be accurately estimated from the image as shown in this study. The most important parameter for LAI determination was the saturated SVI value as the background SVI has a very small effect on the final LAI. The saturated SVI value can be retrieved from the image particularly from large swath imagery, during the growing season.

5. CONCLUSIONS AND FUTURE PROSPECTS

Remote sensing is perhaps the only way to study the status, condition, extent, and dynamics of vegetation at multiple scales because observations can be obtained over large areas of extent with high rate of recurrence. Leaf area index (LAI) is a key vegetation parameter for global and regional models of biosphere-atmosphere exchange of carbon dioxide, nutrients, water vapour, and energy. Retrieval of LAI by means of optical observations constitutes a major challenge to the modern remote sensing techniques.

The main purpose of this dissertation was to enhance the determination of LAI using close-range remote sensing (hemispherical photography), airborne remote sensing (high resolution colour and colour infrared imagery), and satellite remote sensing (high resolution SPOT 5 HRG imagery) optical observations. The commonly used light extinction models were applied at all levels of optical observations. The study areas were Taita Hills, South-East Kenya (I–III) and Gatineau Park, Southern Quebec, Canada (IV–VII). The main findings of this study are as follows:

- Sampling of gap fraction for estimating leaf area and clumping indices from hemispherical photograph is one of the most crucial steps for enhancement of LAI determination. LAI and clumping index estimates are significantly affected by the variation of the size of sky segments for given zenith angle ranges in clumped foliage (I). A new approach to solve the problem of 'empty segments', obscured completely by foliage by merging with the following non-empty segments, is proposed. Theoretically sound and preferred hemisphere region for gap fraction sampling for reliable estimates of LAI and other canopy structure paramaters were demonstrated.
- On sloping ground, LAI and clumping index should be estimated from levelled acquisition (II; III). The tilted acquisition is challenging to setup in the field, makes interpretation of leaf angles complicated, and makes the computation of photosynthetically active radiation (PAR) interception from hemispherical photography difficult. Further studies should look the response of leaf angles to varying slope.
- On a hemispherical photograph taken normal to a horizontal surface (optical axis oriented to local zenith) on sloping ground, gap fractions and size distributions present strong upslope/downslope asymmetry of foliage elements and consequently clumping index estimates (II; III). Both simulated and real photographs analysis demonstrated that the combination of logarithmic gap averaging and gap size distribution approach is performed best (III). This approach was less affected by slope and forest density compared to approaches based on solely logarithmic gap averaging techniques.

- The simulated datasets indicated that several SVIs can be used for LAI mapping provided that the *S* function results are large enough (IV). Further research is required to apply the sensitivity analysis aiming at mapping LAI in vegetation growing on varying soil conditions with a wide range of LAI and f_c. A statistically robust and physically meaningful sensitivity function is still required for use of empirical modelling.
- LAI can be estimated nonparametrically from the information contained solely on the remotely sensed dataset given that the saturated SVI value is accurately determined (V–VII). The logarithmic averaging of gap fraction obtained from remotely sensed data can be used to address quantitatively the scaling issues between different resolutions of spectral data. However, further study is still required to devise a methodology as well as instrumentation to retrieve on-ground 'green leaf area index'. Subsequently, the large scale LAI inversion algorithms presented in this work can be precisely validated.

Based on the literature review and the current study, LAI retrieval from remotely sensed data remains a challenging task. The definition of LAI needs further work and specification. Current validation activities based on the optical field instruments may yield incomparable estimates to those obtained from remotely sensed spectral data (IV-VII). Despite the fact that hemispherical photography was proven to be a powerful technique for determination of LAI as a 'structural' variable, its use is limited by *2D* space information which is used to deal with complex 3D canopy architecture. Is LAI, which is potentially obtainable from top-of-canopy remotely sensed spectral data, a geometrical (structural) and/or biochemical property? Are single view angle remote sensing datasets capable of determining both geometrical and/or biochemical properties of LAI? These issues need further research.

REFERENCES

Abuelgasim AA, RA Fernandas & SG Leblanc (2006). Evaluation of national and global LAI products derived from optical remote sensing instruments over Canada. *IEEE Transactions on Geoscience and Remote Sensing* 44, 1872−1883.

Anderson MC (1964). Studies of the wood-land light climate I. The photographic computation of light condition. *Journal of Ecology* 52. 27−41.

Anderson MC (1971). Radiation and crop structure. *In* Sestak Z, Catsky J, Jarvis PG (eds.): *Plant photosynthetic production: manual of methods,* 412−466. W. Junk, The Hague

Arai K (2000). *Lecture note on Remote Sensing*. Morikita-Shuppan Co., Ltd.

Asner GP, JMO Scurlock & JA Hicke (2003). Global synthesis of leaf area index observations: Implications for ecological and remote sensing studies. *Global Ecology and Biogeography* 12, 191 – 205.

Bacour C, F Baret, D Beal, M Weiss & K Pavageau (2006) .Neural network estimation of LAI, fAPAR, fCover and LAIxCab, from top of canopy MERIS reflectance data: Principles and validation. *Remote Sensing of Environment* 105, 313–325.

Barclay, H.J. (1998) Conversion of total leaf area to projected leaf area in lodgepole pine and Douglas-fir. *Tree Physiology* 18, 185–193.

Barclay HJ & D Goodman (2000). Conversion of total to projected leaf area index in conifers. *Canadian Journal of Botany* 78, 447–454.

Barclay HJ & JA Trofymow (2000). Relationship of readings from the LI-COR canopy analyser to total one-sided leaf index and stand structure in immature Douglas-fir. *Forest Ecology and Management* 132, 121–126.

Baret F & G Guyot (1991). Potentials and limits of vegetation indices for LAI and APAR assessment. *Remote Sensing of Environment* 35, 161−173.

Baret F, O Hagolle, B Geiger, P Bicheron, B Miras, M Huc, B Berthelot, F Nino, M Weiss, O Samain, JL Roujean & M Leroy (2007). LAI, FAPAR, and FCover CYCLOPES global products derived from Vegetation. Part 1: principles of the algorithm. *Remote Sensing of Environment* 110, 305–316.

Barrett EC & LF Curtis (1976). *Introduction to environmental remote sensing.* 336 p. Chapman and Hall, London.

Becker F & BJ Choudhury (1988). Relative sensitivity of normalized difference vegetation index (NDVI) and microwave polarization difference index (MPDI) for vegetation and desertification monitoring. *Remote Sensing of Environment* 24, 297−311.

Berterretche M, AT Hudak, WB Cohen, TK Maiersperger, ST Gower & JL Dungan (2005). Comparison of regression and geostatistical methods for mapping Leaf Area Index (LAI) with Landsat ETM+ data over a boreal forest. *Remote Sensing of Environment* 96, 49–61.

Black TA, JM Chen, XH Lee & RM Sagar (1991). Characteristics of shortwave and longwave irradiances under douglas-fir forest stand. *Canadian Journal of Forest Research* 21, 1020−1028.

Borel C, S Gerstl & B Powers (1991). The radiosity method in optical remote sensing of structured 3D surfaces. *Remote Sensing of Environment* 36, 13–44.

Bowker DE, RE Davis, DL Myrick, K Stacy & WT Jones (1985). *Spectral reflectances of natural targets for use in remote sensing studies.* 184 p. NASA Reference Publication-1139. NASA Langley Research Centre, Hampton, Virginia.

Breda NJJ (2003). Ground-based measurements of leaf area index: a review of methods, instruments and current controversies. *Journal of Experimental Botany* 54, 2403−2417.

Brown L, JM Chen, SG Leblanc & J Cihlar (2000). A shortwave infrared modification to the simple ratio for LAI retrieval in boreal forests: An image and model analysis. *Remote Sensing of Environment* 71, 16–25.

Buermann W, J Dong, X Zeng, R B Myneni & R E Dickinson (2001). Evaluation of the utility of satellite-based vegetation leaf area index data for climate simulations. *Journal of Climate* 14, 3536–3550.

Cable DR (1958). Estimating surface area of ponderosa pine foliage in central Arizona. *Forest Science* 4, 45–49.

Campbell GS (1986). Extinction coefficients for radiation in plant canopies calculated using an ellipsoidal inclination distribution. *Agricultural and Forest Meteorology* 36, 317–321.

Campbell GS (1990). Derivation of an angle density function for canopies with ellipsoidal leaf angle distribution. *Agricultural and Forest Meteorology* 49, 173–176.

Campbell GS & N Norman (1989). The description and measurement of plant canopy structure. *In* Russel G, Marshall B, Jarvis PG (eds.): *Plant canopies: their growth, form and function,* 1−19. Cambridge University Press, Cambridge.

Campbell JB (2002). *Introduction to remote sensing* (3rd ed.). 621 p. Taylor & Francis, London.

Canham CD, JS Denslow, WJ Platt, JR Runkle, TA Spies & PS White (1990). Light regimes beneath canopies and tree-fall gaps in temperate and tropical forests. *Canadian Journal of Forest Research* 20, 620–631.

Carlson TN & DA Ripley (1997). On the relation between NDVI, fractional vegetation cover, and leaf area index. *Remote Sensing of Environment* 62, 241–252.

Chason JW, DD Baldocchi & MA Huston (1991). A comparison of direct and indirect methods for estimating forest canopy leaf area. *Agricultural and Forest Meteorology* 57, 107–128.

Chege J & B Bytebier (2005). Vegetation structure of four small forest fragments in Taita Hills, Kenya. *Journal of African Natural History* 94, 231–234.

Chen JM (1996). Optically-based methods for measuring seasonal variation in leaf area index in boreal confer stands. *Agriculture and Forest Meteorology* 80, 135–163.

Chen JM & TA Black (1992). Defining leaf area index for non-flat leaves. *Plant, Cell and Environment* 15, 421–429.

Chen JM, TA Black & RS Adams (1991). Evaluation of hemispherical photography for determining plant area index and geometry of a forest stand, *Agricultural and Forest Meteorology 56,* 129−143.

Chen JM & J Cihlar (1995). Quantifying the effect of canopy architecture on optical measurements of leaf area index using two gap size analysis methods. *IEEE Transactions of Geoscience and Remote Sensing* 33, 777–787.

Chen JM & J Cihlar (1996). Retrieving leaf area indices of boreal conifer forests using Landsat TM images. *Remote Sensing of Environment* 55, 153–162.

Chen JM, X Li, T Nilson & A Strahler (2000). Recent advances in geometrical optical modelling and its applications. *Remote Sensing Reviews* 18, 227–262.

Chen JM, J Liu, SG Leblanc, R Lacaze & J-L Roujean (2003). Multi-angular optical remote sensing for assessing vegetation structure and carbon absorption. *Remote Sensing of Environment* 84, 516–525.

Chen JM, G Pavlic, L Brown, J Cihlar, SG Leblanc, HP White, RJ Hall, DR Peddle, DJ King, JA Trofymow, E Swift, J Van der Sanden, & PKE Pellikka (2002). Derivation and validation of Canada-wide coarse-resolution leaf area index maps using high resolution satellite imagery and ground measurement. *Remote Sensing of Environment* 80, 165–184.

Chen JM, PM Rich, ST Gower, JM Norman & S Plummer (1997). Leaf area index of boreal forests: Theory, techniques, and measurements. *Journal of Geophysical Research-Atmospheres* 102, 29429−29443.

Cherry M, A Hingston, M Battaglia & C Beadle (1998). Calibrating the LI-COR LAI-2000 for estimating leaf area index in the eucalypt plantations. *Tasforests* 10, 75–82.

Clevers J (1989). The application of a weighted infra-read vegtation index for estimating leaf area index by correcting for soil moisture. *Remote Sensing of Environment* 29, 25−37.

Colombo R, D Bellingeri, D Fasolini & CM Marino (2003). Retrieval of leaf area index in different vegetation types using high resolution satellite data. *Remote Sensing of Environment 86,* 120−131.

Combal B, F Baret, M Weiss, A Trubuil, D Macé, A Pragnère, R Myneni, Y Knyazikhin & L Wang (2002). Retrieval of canopy biophysical variables from bidirectional reflectance using prior information to solve the ill-posed inverse problem. *Remote Sensing of Environment 84*, 1−15.

Coppin PR & ME Bauer (1994). Processing of multitemporal Landsat TM imagery to optimize extraction of forest cover change features. *IEEE Transactions on Geoscience and Remote Sensing* 32, 918−927.

Crabtree R, CS Potter, RS Mullen, J Sheldon, S Huang, J Harmsen, A Rodman & C Jean (2009). Synthesis of ground and remote sensing data for monitoring ecosystem functions in the Colorado River Delta, Mexico, *Remote Sensing of Environment* 113, 1486–1496.

Curran PJ & A Hay (1986). The importance of measurement error for certain procedures in remote sensing at optical wavelengths. *Photogrammetric Engineering and Remote Sensing* 52, 229–241.

Dawson TP, PJ Curran & SE Plummer (1998). LIBERTY – Modeling the effets of leaf biochemical concentration on reflectance spectra. *Remote Sensing of Environment* 65, 50–60.

Demarez V, S Duthoit, F Baret, M Weiss & G Dedieu (2008). Estimation of leaf area and clumping indexes of crops with hemispherical photographs. *Agricultural and Forest Meteorology* 148, 644 – 655.

Dufrêne E & N Bréda (1995). Estimation of deciduous forest leaf area index using direct and indirect methods. *Oecologia*, 104, 156 – 162.

Easter MJ & TA Spies (1994). Using hemispherical photography for estimating photosynthetic photon flux density under canopies and in gaps in Douglas-fir forests of the Pacific Northwest. *Canadian Journal of Forest Research* 24, 2050–2058.

Engman ET (1995). Recent advances in remote sensing in hydrology. *Reviews of Geophysics* 33, 967–976.

Elvidge CD, & C Zhikang (1995). Comparison of Broad-Band and Narrow-Band Red and Near-Infrared Vegetation Indices. *Remote Sensing of Environment* 54, 38−48.

Fang H & S Liang (2005). A hybrid inversion method for mapping leaf area index from MODIS data: experiments and application to broadleaf and needleleaf canopies. *Remote Sensing of Environment* 94, 405–424.

Fernandes R, C Butson, S Leblanc & R. Latifovic (2003). Landsat-5 TM and Landsat-7 ETM+ based accuracy assessment of leaf area index products for Canada derived from SPOT-4 VEGETATION data. *Canadian Journal of Remote Sensing* 29, 241–258.

Fernandes R & SG Leblanc(2005). Parametric (modified least squares) and non-parametric (Theil-Sen) linear regressions for predicting biophysical parameters in the presence of measurement errors. *Remote Sensing of Environment* 95, 303–316.

Fernandes RA, JR Miller, JM Chen & IG Rubinstein (2004). Evaluating image-based estimates of leaf area index in boreal conifer stands over a range of scales using high-resolution CASI imagery. *Remote Sensing of Environment* 89, 200-216.

Fournier RA, R Landry, NM August, G Fedosejevs & RP Gauthier (1996). Modelling light obstruction in tree conifer forests using hemispherical photography and fine tree architecture. *Agricultural and Forest Meteorology* 82, 47–72.

Fournier, RA, PM Rich & R Landry (1997). Hierarchical characterization of canopy architecture for boreal forest. *Journal of Geophysical Research – Atmospheres* 102, 29445–29454

Frazer GW, JA Trofymov & KP Lertzman (1997). *A method for estimating canopy openness, effective leaf area index, and photosynthetically active photon flux density using hemispherical photography and computerized image analysis technique.* 73 p. Natural Resources Canada, Canadian Forestry Service, Forest Ecosystem Processes Network, Pacific Forestry Centre, Information Report BC-X-373.

Ganapol BD, LF Johnson, PD Hammer, CA Hlavka & DL Peterson (1998). LEAFMOD: a new within-leaf radiative transfer model. *Remote Sensing of Environment* 63, 182–193.

García-Haro FJ, MA Gilabert & J Meliá (1999). A radiosity model for heterogeneous canopies in remote sensing. *Journal of geophysical research* 104, 12159–12175.

Garrigues S, NV Shabanov, K Swanson, JT Morisette, F Baret & RB Myneni (2008). Intercomparison and sensitivity analysis of Leaf Area Index retrievals from LAI-2000, AccuPAR, and digital hemispherical photography over croplands. *Agricultural and Forest Meteorology* 148, 1193−1209.

Gastellu-Etchegorry JP, V Demarez, V Pinel & F ZAGOLSKI (1996). Modeling radiative transfer in heterogeneous 3-D vegetation canopies. *Remote Sensing of Environment* 58, 131–156.

Gates DM (1970). Physical and physiological properties of plants. *In* Committee on Remote Sensing for Agricultural Purposes: *Remote Sensing With Special Reference to Agriculture and Forestry*, 224–252. National Academy of Sciences, Washington, DC.

Gates DM, HJ Keegan, JC Schleter & VR Weidner (1965). Spectral properties of plants. *Applied Optics* 4, 11–20

GCOS (2004). *Implementation plan for the Global Observing System for Climate in support of the UNFCCC.* 136 p. Report GCOS – 92 (WMO/TD No. 1219).

GCOS (2008). *Future climate change research and observations: Global Climate Observing System (GCOS), World Climate Research Programme (WCRP) and International Geosphere-Biosphere Programme (IGBP) learning from the Intergovernmental Panel on Climate Change (IPCC).* 68 p. Fourth Assessment Report—Workshop and Survey Report, Sydney, GCOS-117.

Gitelson AA (2004). Wide dynamic range vegetation index for remote quantification of biophysical characteristics of vegetation. *Journal of Plant Physiology* 161, 165−173.

Gobron N & MN Verstraete (2008). *ECV T11: Leaf Area Index (LAI). Assessment of the status of the development of standards for the Terrestrial Essential Climate Variables*. 24 p. Global Terrestrial Observing System, Rome.

Goel N, I Rozehnal & R Thompson (1991). A computer graphics based model for scattering from objects of arbitrary shapes in the optical region. *Remote Sensing of Environment* 36, 73–194

Goetz AFH, JB Wellman & WL Barnes (1985). Optical remote sensing of the earth. *Proceedings of the IEEE* .73, 950−969.

Gonsamo Gosa A, G Schaepman-Strub, L Kooistra, M Schaepman & P Pellikka (2007). Estimation of leaf area index using optical field instruments and imaging spectroscopy. *Proceedings of the 5th EARSeL Workshop on Imaging Spectroscopy*, 23−25 April, Bruges, Belgium.

Govaerts Y & MM Verstraete (1998). Raytran: a Monte Carlo ray-tracing model to compute light scattering in three-dimensional heterogeneous media. *IEEE Transactions on Geoscience and Remote Sensing* 36, 493–505.

Grace J (1987). Theoretical ratio between "one-sided" and total surface area for pine needles. *New Zealand Journal of Forest Science* 17, 292–296.

Gutman G & A Ignatov (1998). The derivation of the green vegetation fraction from NOAA/AVHRR data for use in numerical weather prediction models. *International Journal of Remote sensing* 19, 1533−1543.

Hall FG, YE Shimabukuro, & KF Huemmrich (1995). Remote sensing of forest biophysical structure using mixture decomposition and geometric reflectance models. *Ecological Applications* 4, 993–1013.

Haboudane D, JR Miller, E Pattey, PJ Zarco-Tejada & IB Strachan (2004). Hyperspectral vegetation indices and novel algorithms for predicting green LAI of crop canopies: Modeling and validation in the context of precision agriculture. *Remote Sensing of Environment* 90, 337−352.

Hardisky MA, V Klemas & RM Smart (1983). The influences of soil salinity, growth form, and leaf moisture on the spectral reflectance of *Spartina alterniflora* canopies. *Photogrammetric Engineering and Remote Sensing* 49, 77– 83.

Heinsch FA, M Zhao, SW Running, JS Kimball, RR Nemani, KJ Davis, PV Bolstad, BD Cook, AR Desai, DM Ricciuto, BE Law, WC Oechel, HJ Kwon, H Luo, SC Wofsy, AL Dunn, JW Munger, DD Baldocchi, L Xu, DY Hollinger, AD Richardson, PC Stoy, MBS Siqueira, RK Monson, SP Burns & LB Flanagan (2006). Evaluation of remote sensing based terrestrial productivity from MODIS using regional tower eddy flux network observations. *IEEE Transactions on Geoscience and Remote Sensing* 44, 1908–1925.

Heiskanen J (2006). Estimating aboveground tree biomass and leaf area index (LAI) in a mountain birch forest using ASTER satellite data. *International Journal of Remote Sensing* 27, 1135–1158

Herbert TJ (1987). Area projections of fish-eye lenses, *Agricultural and Forest Meteorology* 39, 215–223.

Hilker T, NC Coops, MA Wulder, AT Black & RD Guy (2008). The use of remote sensing in light use efficiency based models of gross primary production: a review of currant status and future requirements. *Science of the Total Environment* 404, 411–423.

Houborg R, H Soegaard & E Boegh (2007). Combining vegetation index and model inversion methods for the extraction of key vegetation biophysical parameters using Terra and Aqua MODIS reflectance data. *Remote Sensing of Environment 106*, 39−58.

Huang D, Y Knyazikhin, RE Dickinson, M Rautiainen, P Stenberg, M Disney, P Lewis, A Cescatti, Y Tian, W Verhoef, JV Martonchik & RB Myneni (2007). Canopy spectral invariants for remote sensing and model applications. *Remote Sensing of Environment* 106, 106–122.

Huemmrich KF (2001). The GeoSail model: A simple addition to the SAIL model to describe discontinuous canopy reflectance. *Remote Sensing of Environment* 75, 423–431

Huete A, C Justice & H Liu (1994). Development of vegetation and soil indices for MODIS-EOS. *Remote Sensing of Environment* 49, 224−234.

Hurk BJJM van den, P Viterbo & S Los (2003). Impact of Leaf Area Index seasonality on annual land surface evaporation in a Global Circulation Model. *Journal of Geophysical research* 108, 4191−4199.

Jacquemoud S, C Bacour, H Poilvé & J-P Frange (2000). Comparison of four radiative transfer models to simulate plant canopies reflectance: direct and inverse mode. *Remote Sensing of Environment* 74, 471–481.

Jacquemoud S & F Baret (1990). PROSPECT: a model of leaf optical properties spectra. *Remote Sensing of Environment* 34, 75–91.

Jacquemoud S, W Verhoef, F Baret, C Bacour, PJ Zarco-Tejada, GP Asner, C Francois & SL Ustin (2009). PROSPECT + SAIL models: A review of use for vegetation characterization. *Remote Sensing of Environment* 113, S56–S66.

Janzen HH (2004). Carbon cycling in earth systems – a soil science perspective. *Agriculture Ecosystems and Environment* 104, 399–417.

Jensen JR (2000). *Remote Sensing of the Environment: An Earth Resource Perspective.* 544 p. Prentice Hall, NJ.

Jensen JR & IM Jungho (2008). Hyperspectral remote sensing of vegetation. *Geography Compass* 6, 1943 – 1961.

Ji L & AJ Peters (2007). Performance evaluation of spectral vegetation indices using a statistical sensitivity function. *Remote Sensing of Environment* 106, 59–65.

Jiang ZY, AR Huete, J Chen, YH Chen, J Li, GJ Yan & XY Zhang (2006). Analysis of NDVI and scaled difference vegetation index retrievals of vegetation fraction. *Remote Sensing of Environment* 101, 366−378.

Johnson JD (1984). A rapid technique for estimating total surface area of Pine needles. *Forest science* 30, 913−921.

Jonckheere I, S Fleck, K Nackaerts, B Muysa, P Coppin, M Weiss & F Baret (2004). Review of methods for *in situ* leaf area index determination Part I. Theories, sensors and hemispherical photography. *Agricultural and Forest Meteorology* 121, 19 – 35.

Jones HG (1992). *Plants and Microclimate. A Quantitative Approach to Environmental Plant Physiology.* 428 p. Cambridge University Press, Cambridge.

Jordan CF (1969). Deviation of leaf area index from quality of light on the forest floor. *Ecology* 50**,** 663−666.

Loveland T, Y Yasuoka, B Burgan, J Chen, R Defries, HG Lund, T Lynham, P Mayaux & J-M Gregoire (1998). *Global Observations of Forest Cover: Coarse Resolution Products Design Strategy*. 23 p. GOFC-GOLD Report No. 3. Sioux Falls, South Dakota, US EROS Data Center.

Kimes DS & JA Kirchner (1982). Radiative transfer model for heterogeneous 3D scenes. *Applied Optics* 21, 4119–4129.

King DJ, I Olthof, PKE Pellikka, ED Seed & C Butson (2005). Modelling and mapping forest ice storm damage using remote sensing and environmental data. *Natural Hazards* 35, 321−342.

Knyazikhin Y, J Glassy, JL Privette, Y Tian, A Lotsch, Y Zhang, Y Wang, JT Morisette, P Votava, RB Myneni, RR Nemani & SW Running (1999). *MODIS Leaf Area Index (LAI) and Fraction of Photosynthetically Active Radiation Absorbed by Vegetation (FPAR) Product.* Version 4.0(MOD15) Algorithm Theoretical Basis. 130 p. http://modis.gsfc.nasa.gov/data/atbd/atbd_mod15.pdf

Knyazikhin Y, JV Martonchik, RB Myneni, DJ Diner & SW Running (1998). Synergistic algorithm for estimating vegetation canopy leaf area index and fraction of absorbed photosynthetically active radiation from MODIS and MISR data. *Journal of Geophysical Research* 103, 32257–32276.

Kozlowski TT & FX Schumacher (1943). Estimation of stomated foliar surface of pines. *Plant Physiology* 18, 122–127.

Kuusk A (1995). A Markov chain model of canopy reflectance. *Agricultural and Forest Meteorology* 76, 221–236.

Kuusk A (1998). Monitoring of vegetation parameters on large areas by the inversion of a canopy reflectance model. *International Journal of Remote Sensing* 19, 2893-2905.

Kuusk A, J Kuusk & M Lang (2009). A dataset for the validation of reflectance models. *Remote Sensing of Environment* 113, 889−892.

Kuusk A & T Nilson (2000). A directional multispectral forest reflectance model. *Remote Sensing of Environment* 72, 244–252.

Lacaze R, JM Chen, J-L Roujean & SG Leblanc (2002). Retrieval of vegetation clumping index using hot spot signatures measured by POLDER instrument. *Remote Sensing of Environment* 79, 84–95.

Lang ARG (1986). Leaf area and average leaf angle from transmission of direct sunlight. *Australian Journal of Botany* 34, 349–355.

Lang ARG (1987). Simplified estimate of leaf area index from transmittance of the sun's beam. *Agricultural and Forest Meteorology* 41, 179–186.

Lang ARG, RE McMurtrie & ML Benson (1991). Validity of surface area indices of Pinus radiata estimated from transmittance of the sun's beam. *Agricultural and Forest meteorology* 57, 157–170.

Lang ARG & Y Xiang (1986). Estimation of leaf area index from transmission of direct sunlight in discontinuous canopies. *Agricultural and Forest meteorology* 37, 229−243.

Latifovic R & D Pouliot (2007). Analysis of climate change impacts on lake ice phenology in Canada using the historical satellite data record. *Remote Sensing of Environment* 106, 492−507.

Leblanc SG (2002). Correction to the plant canopy gap-size analysis theory used by the tracing radiation and architecture of canopies instrument, *Applied Optics* 31**,** 7667–7670.

Leblanc SG, P Bicheron, JM Chen, M Leroy & J Cihlar (1999). Investigation of directional reflectance in boreal forests with an improved four-scale model and airborne POLDER data. *IEEE Transactions on Geoscience and Remote Sensing* 37, 1396–1414.

Leblanc SG, JM Chen, R Fernandes, DW Deering & A Conley (2005). Methodology comparison for canopy structure parameter extraction from digital hemispherical

photography in boreal forests. *Agricultural and Forest Meteorology* 129, 187–207.

Leblanc SG, JM Chen, PH White, J Cihlar, J-L Roujean & R Lacaze (2001). Mapping vegetation clumping index from directional satellite measurements. *Proceedings of Symposium on Physical Signatures and Measurements in Remote Sensing* 8–13 January, Aussois, France.

Lévesque J & DJ King (1999). Airborne Digital Camera Image Semivariance for Evaluation of Forest Structural Damage at an Acid Mine Site. *Remote Sensing of Environment* 68, 112 – 124.

Li X, AH Strahler & CE Woodcock (1995). A hybrid geometric optical-radiative transfer approach for modelling albedo and directional reflectance of discontinuous canopies. *IEEE Transactions on Geoscience and Remote Sensing* 33, 466–480.

Liang S (2004). *Quantitative Remote Sensing Of Land Surfaces*. 534 p. Wiley Series in Remote Sensing. John Wiley & Sons, Inc.

Liang S, H Fang, L Thorp, M Kaul, TGV Niel, TR McVicar, J Pearlman, C Walthall, C Daughtry, F Huemmrich & DLB Jupp (2003). Estimation and validation of land surface broadband albedos and leaf area index from EO-1 ALI data. *IEEE Transactions on Geoscience and Remote Sensing* 41, 1260–1267.

LI-COR (1992). *LAI-2000 Plant Canopy Analyser*. Instruction Manual. LICOR, Lincoln, NE, USA.

Lintz J & DS Simonett (1976). *Remote Sensing of the Environment.* 713 p. Addison-Wesley, Reading, Massachusetts.

Los SO, GJ Collatz, PJ Sellers, CM Malmstroem, NH Pollack, RS DeFries, L Bounoua, MT Parris, CJ Tucker & DA Dazlich (2000). A global 9-year biophysical land surface data set from NOAA AVHRR data. *Journal of Hydrometeorology 1*, 183–199.

Macfarlane C, A Grigg & C Evangelista (2007). Estimating forest leaf area using cover and fullframe fisheye photography: thinking inside the circle. *Agricultural and Forest Meteorology* 146**,** 1–12.

Madgwick HA (1964). Estimation of surface area of pine needles with special reference to *Pinus resinosa*. *Journal of Forestry* 62, 636.

Maier SW, W Lüdeker & KP Günther (1999). SLOP: a revised version of the stochastic model for leaf optical properties. *Remote Sensing of Environment* 68, 273–280.

McWilliam A-LC, JM Roberts, OMR Cabral, MVBR Leitao, ACL de Costa, GT Maitelli & CAGP Zamparoni (1993). Leaf area index and above-ground biomass of terra firme rain forest and adjacent clearings in Amazonia. *Functional Ecology* 7, 310−317.

Miller JB (1967). A Formula for Average Foliage Density. *Australian Journal of Botany* 15, 141–144.

Monteith JL & MH Unsworth (1990). *Principles of Environmental Physics.* 2nd edn. 241 p. Edward Arnold, London.

Myneni RB, S Hoffman , Y Knyazikhin , JL Privette , J Glassy , Y Tian , Y Wang, X Song , Y Zhang , GR Smith , A Lotsch , M Friedl , JT Morisette , P Votava , RR Nemani & SW Running (2002). Global products of vegetation leaf area and fraction absorbed PAR from year one of MODIS data. *Remote Sensing of Environment* 83, 214−231.

Nackaerts K, P Coppin, B Muys & M Hermy (2000). Sampling methodology for LAI measurements with LAI-2000 in small forest stands. *Agricultural and Forest Meteorology* 101, 247–250.

Nemani RR, LL Pierce, SW Running & L Band (1993). Forest ecosystem processes at the watershed scale: Sensitivity to remotely sensed leaf area index estimates. *International Journal of Remote Sensing* 14, 2519–2534.

Neumann HH, G Den Hartog & RH Shaw (1989). Leaf area measurements based on hemispheric photographs and leaf-litter collection in a deciduous forest during autumn leaf-fall. *Agricultural and Forest Meteorology* 45, 325–345.

Nilson T (1971). A theoretical analysis of the frequency of gaps in plant stands. *Agricultural and Forest meteorology* 8, 25–38.

Nilson T (1999). Inversion of gap fraction data in forest stands. *Agricultural and Forest Meteorology* 98/99, 437–448.

Nilson T & A Kuusk (2004). Improved algorithm for estimating canopy indices from gap fraction data in forest canopies. *Agricultural and Forest Meteorology* 124, 157−169.

Nilson T & U Peterson (1991). A forest canopy reflectance model and a test case. *Remote Sensing of Environment* 37, 131–142.

Norman JM & GS Campbell (1989). Canopy structure. *In* Pearcy RW, Ehleringer J, Mooney HA, Rundel PW (eds.): *Plant physiological ecology: field methods and instrumentation,* 301−325. Chapman and Hall, NewYork.

North PRJ (2002). Estimation of fAPAR, LAI, and vegetation fractional cover from ATSR-2 imagery. *Remote Sensing of Environment* 80, 114−121.

Olthof I, DJ King & RA Lautenschlager (2001). Leaf area index change in ice-storm damaged sugar maple stands. *The Forestry Chronicle* 77, 627−635.

Olthof I, DJ King & RA Lautenschlager (2003). Overstory and understory leaf area index as indicators of forest response to ice storm damage. *Ecological Indicators* 3, 49−64.

Olthof I, DJ King & RA Lautenschlager (2004). Mapping deciduous forest ice storm damage using Landsat and environmental data. *Remote Sensing of Environment* 89, 484−496.

Ozanne CMP, D Anhuf, SL Boulter, M Keller, RL Kitching, C Korner, FC Meinzer, AW Mitchell, T Nakashizuka, PL Silva Dias, NE Stork, SJ Wright & M Yoshimura (2003). Biodiversity meets the atmosphere: a global view of forest canopies. *Science* 301, 183–186.

Peddle, DR, SP Brunke & FG Hall (2001). A comparison of spectral mixture analysis and ten vegetation indices for estimating boreal forest biophysical information from airborne data. *Canadian Journal of Remote Sensing* 27, 627–635.

Pasher J & DJ King (2006). Landscape fragmentation and ice storm damage in eastern Ontario forests. *Landscape Ecology* 21, 477−483.

Pellikka P (1998). Development of correction chain for multispectral airborne video camera data for natural resource assessment. *Fennia* 176, 1 – 110.

Pellikka P, DJ King & SG Leblanc (2000a). Quantification and reduction of bidirectional effects in deciduous forest in aerial CIR imagery using two reference land surface types. *Remote Sensing Reviews* 19, 259−291.

Pellikka P, ED Seed & DJ King (2000b). Modelling deciduous forest ice storm damage using aerial CIR imagery and hemispheric photography. *Canadian Journal of Remote Sensing* 26, 394−405.

Pellikka PKE, M Lötjönen, M Siljander & L Lens (2009). Airborne remote sensing of spatiotemporal change (1955−2004) in indigenous and exotic forest cover in the

Taita Hills, Kenya. *International Journal of Applied Earth Observations and Geoinformation* 11, 221−232.
Perry CR & LF Lautenschlager (1984), Functional equivalence of spectral vegetation indices. *Remote Sensing of Environment* 14, 169−182.
Perry SG, AB Fraser, DW Thomson & JM Norman (1988). Indirect sensing of plant canopy structure with simple radiation measurements. *Agricultural and Forest meteorology* 42, 255−278.
Pielou EC (1962). Runs of one species with respect to another in transects through plant populations. *Biometrics* 18, 579–593.
Pierce LL & SW Running (1988). Rapid estimation of coniferous forest leaf area index using a portable integrating radiometer. *Ecology* 69, 762–1767.
Pisaric MFJ, DJ King, AJM MacIntosh & R Bemrose (2008). Impact of the 1998 ice storm on the health and growth of sugar maples (*Acer saccharum* Marsh) dominated forests in Gatineau Park, Quebec. *Journal of the Torrey Botanical Society* 135, 530−539.
Pisek, J & JM Chen (2007). Comparison and validation of MODIS and VEGETATION global LAI products over four BigFoot sites in North America. *Remote Sensing of Environment* 109, 81−94.
Planchais I & JY Pontailler (1999). Validity of leaf areas and angles estimated in a beech forest from analysis of gap frequencies, using hemispherical photographs and a plant canopy analyzer. *Annals of Forest Science* 56, 1–10.
Qi J, A Chehbouni, A Huete, Y, Kerr & S Sorooshian (1994). A modified soil adjusted vegetation index. *Remote Sensing of Environment* 48, 119–126.
Rasmus Houborg R, M Anderson & C Daughtry (2009). Utility of an image-based canopy reflectance modeling tool for remote estimation of LAI and leaf chlorophyll content at the field scale. *Remote Sensing of Environment 113, 259−274.*
Rautiainen M, M Mottus & P Stenberg (2009). On the relationship of canopy LAI and photon recollision probability in boreal forests. *Remote Sensing of Environment* 113, 458–461.
Rautiainen M & P Stenberg (2005). Application of photon recollision probability in coniferous canopy reflectance simulations. *Remote Sensing of Environment* 96, 98–107.
Rich PM (1990). Characterizing plant canopies with hemispherical photographs. *Remote Sensing Review* 5, 13–29.
Rich PM, DB Clark, DA Clark & SF Oberbauer (1993). Long-term study of solar radiation regimes in a tropical wet forest using quantum sensors and hemispherical photography. *Agriculture and Forest Meteorology*. 107–127.
Richardson AJ, CL Wiegand, DF Wanjura, D Dusek & JL Steiner (1992). Multisite analyses of spectral-biophysical data for sorghum. *Remote Sensing of Environment* 41, 71−82.
Rignot E, WA Salas & DL Skole (1997). Mapping deforestation and secondary growth in Rondonia, Brazil, using imaging radar and thematic mapper data. *Remote Sensing of Environment* 59, 167−179.
Rogers PC, B O'Connell, J Mwangombe, S Madoffe & G Hertel (2008). Forest health monitoring in the Ngangao forest, Taita Hills, Kenya: a five year assessment of change. *Journal of East African Natural History* 97, 3–17.
Rondeaux G, M Steven & F Baret (1996). Optimization of soil-adjusted vegetation indices. *Remote Sensing of Environment* 55, 95−107.

Ross J (1981). *The radiation regime and architecture of plant stands*. 420 p. Junk, The Hague

Rouse JW, RH Haas, JA Schell & DW Deering (1973). Monitoring vegetation systems in the Great Plains with ERTS. *Proceeding of Third ERTS Symposium,* 301–319. NASA SP-351 I.

Saatchi SS, JV Soares & DS Alves (1997). Mapping deforestation and land use in Amazon rainforest by using SIR-C imagery. *Remote Sensing of Environment* 59,191−202.

Sasaki T, J Imanishi, K Ioki, Y Morimoto & K Kitada (2008). Estimation of leaf area index and canopy openness in broad-leaved forest using an airborne laser scanner in comparison with high-resolution near-infrared digital photography. *Landscape and Ecological Engineering* 4, 47−55.

Scurlock JMO, GP Asner & S T Gower (2001). *Global Leaf Area Index Data from Field Measurements, 1932-2000.* Oak Ridge National Laboratory Distributed Active Archive Center, Oak Ridge, Tennessee, U.S.A. http://www.daac.ornl.gov

Seed, ED & DJ King (2003). Shadow brightness and shadow fraction relations with effective LAI: Importance of canopy closure and view angle in mixedwood boreal forest. *Canadian Journal of Remote Sensing*, 29, 324–335.

Shunlin L & H Fang (2004). A hybrid inversion method for mapping leaf area index from MODIS data: experiments and application to broadleaf and needleleaf canopies. *Remote Sensing of Environment* 94, 405–424.

Slaton MR, ER Hunt Jr. & WK Smith (2001).Estimating near-infrared leaf reflectance from leaf structural characteristics. *American Journal of Botany* 88, 278−284.

Smith NJ, JM Chen & TA Black (1993). Effects of clumping on estimates of stand leaf area index using the LI-COR LAI-2000. *Canadian Journal of Forest Research* 23, 1940–1943

Song C, CE Woodcock, KC Seto, M Pax Lenney & SA Macomber (2001). Classification and change detection using Landsat TM data: when and how to correct atmospheric effects? *Remote Sensing of Environment* 75, 230–244.

Soudani K, C Francois, G le Maire, V Le Dantec & E Dufrene (2006). Comparative analysis of IKONOS, SPOT, and ETM+ data for leaf area index estimation in temperate coniferous and deciduous forest stands. *Remote Sensing of Environment* 102, 161−175.

Stenberg P (1996a). Correcting LAI-2000 estimates for the clumping of needles in shoots of conifers. *Agricultural and Forest Meteorology* 79, 1-8.

Stenberg P (1996b). Simulations of the effects of shoot structure and orientation on vertical gradients in intercepted light by conifer canopies. *Tree Physiology* 16, 99–108.

Stenberg P (2006). A note on the G-function for needle leaf canopies. *Agricultural and Forest Meteorology* 136, 76−79.

Stenberg P (2007). Simple analytical formula for calculating average photon recollision probability in vegetation canopies. *Remote Sensing of Environment* 109, 221–224.

Stenberg P, S Linder, H Smolander & J Flower-Ellis (1994). Performance of the LAI-2000 plant canopy analyser in estimating leaf area index of some Scots pine stands. *Tree Physiology* 14, 981–995.

Stenberg P, M Rautiainen, T Manninen, P Voipio & M Mõttus (2008). Boreal forest leaf area index from optical satellite images: model simulations and empirical analyses using data from central Finland. *Boreal Environment Research* 13, 433−443.

Stenberg P, M Rautiainen, T Manninen, P Voipio & H Smolander (2004). Reduced simple ratio better than NDVI for estimating LAI in Finnish pine and spruce stands. *Silva Fennica* 38, 3–14.

Stern WR & CM Donald (1961). Relationship of Radiation, Leaf Area Index and Crop Growth-Rate. *Nature* 189, 597 − 598

Suits GH (1972). The calculation of the directional reflectance of a vegetative canopy. *Remote Sensing of Environment* 2, 117–125.

Suits GH (1973).The cause of azimuthal variations in directional reflectance of vegetative canopies. *Remote Sensing of Environment* 2, 175−182.

Sun G & KJ Ranson (1995). A three-dimensional radar backscatter model of forest canopies. *IEEE Transactions on Geoscience and Remote Sensing* 33, 372–382.

Sun G & KJ Ranson (2000). Modeling lidar returns from forest canopies. *IEEE Transactions on Geoscience and Remote Sensing* 38, 2617-2626.

Tucker CJ (1979). Red and photographic infrared linear combinations for monitoring vegetation. *Remote Sensing of Environment* 8, 127−150.

Tucker CJ & MW Garratt (1977). Leaf optical system modeled as a stochastic process. *Applied Optics* 16, 635−642.

Ustin SL, PG Valko, SC Kefauver, MJ Santos, JF Zimpfer & SD Smith (2009). Remote sensing of biological soil crust under simulated climate change manipulations in the Mojave Desert. *Remote Sensing of Environment* 113, 317−328.

van Gardingen PR, GE Jackson, S Hernandez-Daumas, G Russell & L Sharp (1999). Leaf area index estimates obtained for clumped canopies using hemispherical photography. *Agricultural and Forest Meteorology* 94, 243−257.

Verhoef W (1984). Light scattering by leaf layers with application to canopy reflectance modelling: the SAIL model. *Remote Sensing of Environment* 16, 125–141.

Vermote EF, D Tanré, JL Deuzé, M Herman & JJ Morcrette (1997). Second simulation of the satellite signal in the solar spectrum, *6S*: an overview. *IEEE Transactions on Geoscience and Remote Sensing* 35, 675–686.

Verstraete MM & B Pinty (1991). The potential contribution of satellite remote sensing to the understanding of arid lands processes. *Vegetation* 91, 59–72.

Vickery PJ, IL Bennett & GR Nicol (1980). An improved electronic capacitance meter for estimating herbage mass. *Grass Forage Science* 35, 247–252.

Walter J-MN (2008). *Hemispherical Photography of Forest Canopies. A Package of Programs for the Assessment of Canopy Geometry and Solar Radiation Regimes through Hemispherical Photographs.* Université de Strasbourg, France.

Walter J-MN & EF Torquebiau (2000). The computation of forest leaf area index on slope using fish-eye. *Comptes Rendus de l'Acade´mie des Sciences, Se´rie III. Sciences de la Vie* 323, 801−813.

Walter J-MN, RA Fournier, K Soudani & E Meyer (2003). Integrating clumping effects in forest canopy structure: An assessment through hemispherical photographs. *Canadian Journal of Remote Sensing* 29, 388–410.

Waring RH (1985). Imbalanced forest ecosystems: assessments and consequences. *Forest Ecology and management* 12, 93−112.

Waring RH, PE Schroeder & R Oren (1982). Application of the pipe model theory to predict canopy leaf area. *Canadian Journal of Forest Research* 12, 556–560.

Warren-Wilson J & JE Reeve (1959). Analysis of the spatial distribution of foliage by two-dimensional point quadrats. *New Phytologist* 58, 92−101.

Watson, D (1947). Comparative physiological studies in the growth of field crops. I.Variation in net assimilation rate and leaf area between species and varieties, and within and between years. *Annals of Botany 11*, 41−76.

Weiss M, F Baret, GJ Smith, I Jonckheere & P Coppin (2004). Review of methods for *in situ* leaf area index (LAI) determination: Part II. Estimation of LAI, errors and sampling. *Agricultural and Forest Meteorology* 121, 37–53.

Welles JM (1990). Some indirect methods of estimating canopy structure. *Remote Sensing Review* 5, 31–43.

White LP (1977). *Aerial photography and remote sensing for soil survey.* 104 p. Clarendon Press, New York.

Whitford KR, IJ Colquhoun, ARG Lang & BM Harper (1995). Measuring leaf-area index in a sparse eucalypt forest—A comparison of estimates from direct measurement, hemispherical photography, sunlight transmittance and allometric regression. *Agricultural and Forest Meteorology* 74, 237–249.

Widlowski J-L**,** Robustelli M, M Disney, J-P Gastellu-Etchegorry, T Lavergne, P Lewis, PRJ North, B Pinty, R Thompson & MM Verstraete (2008). The RAMI On-line Model Checker (ROMC): A web-based benchmarking facility for canopy reflectance models. *Remote Sensing of Environment* 112, 1144–1150.

Wiegand CL, AH Gerberman, KP Gallo, BL Blad & D Dusek (1990). Multisite analyses of spectral-biophysical data for corn. *Remote Sensing of Environment* 33, 1−16.

Wiegand CL, SJ Maas, JK Aase, JL Hatfield, PJ Pinter, Jr. RD Jackson, ET Kanemasu & RL Lapitan (1992). Multisite analysis of spectral-biophysical data for wheat. *Remote Sensing of Environment* 42, 1−22.

Wilson JW (1960). Inclined point quadrats. *New Phytologist* 59, 1–8.

Wulder MA & SE Franklin (2003). *Remote Sensing of Forest Environments: Concepts and Case Studies.* 552 p. Kluwer Academic Publishers, Boston.

Yang W, B Tan, D Huang, M Rautiainen, NV Shabanov, Y Wang, JL Privette, KF Huemmrich, R Fensholt, I Sandholt, M Weiss, DE Ahl, ST Gower, RR Nemani, Y Knyazikhin & RB Myneni (2006). MODIS leaf area index products: From validation to algorithm improvement. *IEEE Transactions on Geoscience and Remote Sensing* 44, 1885 – 1899.

Zhang YQ, F HS Chiew, L Zhang, R Leuning & HA Cleugh (2008). Estimating catchment evaporation and runoff using MODIS leaf area index and the Penman-Monteith equation. *Water Recourse Research* 44, W10420.1−W10420.15.